Turkish Journal of Engineering
https://dergipark.org.tr/en/pub/tuje
e-ISSN 2587-1366

Geo-Appraisal of groundwater resource for sustainable exploitation and management in Ibulesoro, Southwestern Nigeria

Olumuyiwa Olusola Falowo [*1], **Abayomi Solomon Daramola** [1]

[1] *Rufus Giwa Polytechnic Owo, Ondo State, Department of Civil Engineering Technology, Nigeria*

Keywords
Ibulesoro
Irrigation indices
Water quality index
Groundwater exploration
GWPIV

Research Article
DOI: 10.31127/tuje.1107329

Received: 22.04.2022
Accepted: 03.08.2022
Published: 31.08.2022

Abstract

Groundwater exploitation requires better understanding of the resource availability and quality/vulnerability. Geophysical techniques, pumping test, hydraulic measurement, borehole logging and quality test analysis have been used in Ibulesoro, southwestern Nigeria, to understanding the hydrogeological system in terms of groundwater availability, aquifer delineation, and evaluate the groundwater physico-chemical and biological contents. The study utilized multi-criteria evaluation techniques (GWPIV) to assess the overall aquifer potential/vulnerability. The geology of the area comprises granite, migmatite, migmatite gneiss, biotitic granite, and gneiss. The main water-bearing unit was the weathered layer and fractured basement, which are usually unconfined aquifer. The hydraulic conductivity and formation factor is related by $y = 0.239e^{0.0519x}$ with correlation coefficient of 0.0961. The average hydraulic conductivity and transmissivity are 0.52 m/d and 5.78 m^2/d respectively. The hydrogeological parameters viability increases southwardly, just as groundwater movement/flow is due south. The average thickness of the weathered layer and overburden are 8.6 m and 16.1 m respectively, with dominant resistivity in the range of 80 – 200 ohm-m. The best drilling points (migmatite/gneiss geologic units) are where the fractured basement underlies the weathered layer which most not necessarily exceed 30 - 35 m. The average depth to basement rock is 16.1 m. The obtained GWPIV varied from 1.12 to 1.71, with an average of 1.30 suggesting low potential but good for drinking and irrigation uses in its present state, however highly vulnerability to contamination, as the vadose zone thickness (5.68 m avg.), AVI (0.57 avg.), and LC (0.0818 mhos avg.) all point to the low protective capability. The water types is mixed Ca-Mg-Cl. The mechanism controlling the groundwater quality falls in the mixed zone, which indicates contribution from soil/rock-water interaction, precipitation, and evaporation; while carbonic weathering is more active than the silicate weathering process.

1. Introduction

Advancement and management of groundwater resources is becoming critical in the face of worldwide water scarcity challenges [1]. Ibulesoro is one of the fastest-growing towns in Ondo State's Ifedore Local Government Area in terms of infrastructure, health facilities, housing and estate development, groundwater development, and the emergence of small/micro businesses and industries in the previous ten years. As a result of the boundary shared with FUTA, the staff prefer settling down in the town, hence the population of the town is growing geometrically. However, due to a lack of treated water from a government-owned well, many residents in the town rely on shallow wells/borehole. But data on these boreholes are usually not available, since many don't carry out hydrogeological survey before drilling operation, which generally leads to unsuccessful/failed boreholes. These abandoned boreholes are typically not backfilled, and they might serve as a route for contaminants to reach an aquifer (if the not cased). For solid and liquid wastes, many have turned to waste disposal sites, which pose a clear threat to water quality. This can lead to ground subsidence, landslides, and other issues. As a result, water resource development and management need to take operate

* **Corresponding Author**
*(solageo2018@gmail.com) ORCID ID 0000-0003-3425-9072
(yomidams02@gmail.com) ORCID ID 0000-0002-0309-2399

Cite this article
Falowo, O. O., Daramola, A. S. (2023). Geo-Appraisal of groundwater resource for sustainable exploitation and management in Ibulesoro, Southwestern Nigeria. Turkish Journal of Engineering, 7(3), 236-258

within a framework of legitimate duties, privileges, and limits [2]. The study's goals were to identify and delineate geological sequences and factors in terms of capacity and value with the mandate to improving groundwater management and development. This study used a combination of geoelectric measures, hydrogeological, borehole logging, and groundwater quality to define the current state of the aquifer system in the area for drinking and irrigation uses [3-4]. Since aquifer permeability, underlying strata lithology, temporal variations in the source and configuration of recharged water, hydrology, and human impacts all influence the occurrence and movement of groundwater resources [5-8].

For decades, the mining and petroleum industries have relied on geophysical surveys. This survey's utility has been demonstrated in the exploration of shallow near-surface/subsurface groundwater supplies [9-13]. The most frequent approaches are dc resistivity, seismic refraction, and gravity and magnetics methods [14-16]. The magnitude and character of the geologic resources below the surface can be determined indirectly using geophysical methods. The depth to/of the basement rocks, as well as the thickness of subsurface faults. Dc electrical resistivity (ER) is the most widely used of the several electrical geophysical methods in hydrogeology [7,17,18]. The ER is a direct current that is delivered to the ground via two metal electrodes. The ground voltage is measured between two metal electrodes that are also driven in the ground. The resistivity of the earth materials between the electrodes can be calculated by the current flowing through the ground and the potential differences or voltage between the electrodes. The expression in equation 1 equals electrical resistivity (R).

$$R = \frac{A}{L}\frac{\Delta V}{I} \tag{1}$$

A = Cross sectional area of current flow
L = Length of the flow path
ΔV = Voltage drop
I = Electrical current

The unit of ER is in ohm-m or ohm-ft units. The four electrodes utilized are: A- +current electrode, B is -current electrode, M-potential electrodes, and N-potential electrodes. If XY denotes the distance between Electrode X and Electrode Y, equation (1) can be written as:

$$R = \left(\frac{2\pi}{\frac{1}{AM} - \frac{1}{BM} - \frac{1}{AN} + \frac{1}{BN}}\right)\frac{\Delta V}{I} \tag{2}$$

The resistivity derived in equation 2 is an apparent resistivity (R) because the earth materials are nearly homogeneous and electrically isotropic. Schlumberger array arrangement is employed in this investigation. It's a linear array of close-together potential electrodes. AB is usually configured to be equal to or larger than five times MN. Equation (3) gives the apparent resistivity:

$$R = \frac{\pi\left(\left(\frac{AB}{2}\right)^2\right) - \left(\left(\frac{MN}{2}\right)^2\right)}{MN}\frac{\Delta V}{I} \tag{3}$$

The electrical sounding indicates the depth-dependent differences in apparent resistance. The distance between the potential electrodes and the current electrodes increases as the electrode spacing is increased in electrical sounding. This implies deeper penetration of current into the earth, measuring apparent resistance as it does so.

Hydraulic characteristics of earth materials and groundwater are typically determined in hydrogeological research [19]. This usually entails digging exploratory wells and observing and analyzing pumping test data in order to calculate hydraulic conductivity, transmissivity, storability, safe yields, and hydraulic gradient, among other things. The goal of an exploratory well is to gather data on the geology of the subsurface aquifer. Aquifer tests are often used to analyze the physical qualities of aquifers, in addition to reporting the various geological layers encountered (well logs). Step-down tests are frequently performed before these tests to know the appropriate discharge rate. As a result, one of the focuses of this study is the ability to pump the required volume of water at the lowest cost, taking into account investment, operation, and maintenance [20-21].

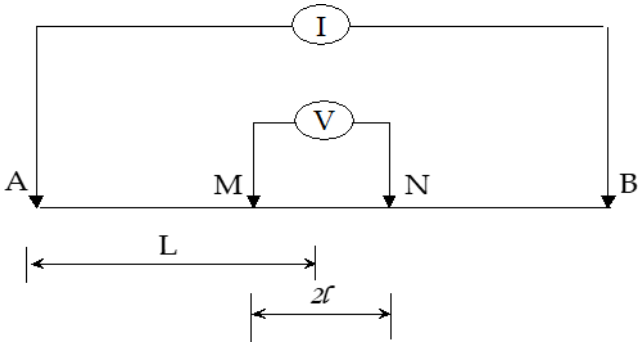

Figure 1. Schlumberger Electrode Configuration.

Safeguarding the water quality in an aquifer is a crucial aspects of groundwater management, and this is done by determining the vulnerability potential [22] from septic tanks, sanitary landfills, municipal wastewater land treatment systems, waste injection wells, toxic chemical disposal sites, cemeteries, mine tailings, mine drainage, water softener regeneration salts, oil field brine, agricultural chemicals and fertilizers, and accidental oil [23-27]. Several approaches for assessing aquifer vulnerability have been presented; among these, index methods such as DRASTIC, GOD, and IRIH are the most extensively utilized [28-29]. S-model aquifer vulnerability assessment is a less expensive option to index models. The protective capacity of the vadose zone is examined in the S-model (e.g., AVI, LC, etc.) by defining the lithological configuration and depth using ER sounding. Because of the development of computer programs, electrical resistivity, which involves the computation of longitudinal conductance, is now used in groundwater research [30]. Furthermore, the water quality index (WQI) is gaining in favor around the

world for monitoring groundwater quality [26,31-34]. The water quality index describes the quality of water in terms of an index number that shows the water's complete quality for any anticipated purpose. It's a mathematical method for changing vast quantities of data on water quality into a distinct number that specifies the water quality level. In fact, establishing WQI in a given area is an important step in land use and water resource management planning. Typically, WQI is calculated from the standpoint of its appropriateness for human drinking.

Aquifers can play a variety of roles in the general development of a region's water resources, including supplying water to wells (supply function) and transporting water from one point to another (pipeline function). An aquifer's unsaturated zone can serve as a waste treatment system. This is known as the aquifer's filter-plant function [35-36]. The unsaturated zone, on the other hand, can do greatly more than serve as a physical filter for germs and viruses. Heavy metals and phosphorus are also effectively removed. Water can also be improved by passing through the saturated zone. Groundwater can serve as an energy source (groundwater heat pump) as well as a storage medium [37].

Groundwater contamination or susceptibility has recently piqued the interest of many researchers throughout the world [16,38-44], because of the significance role it plays in overall wellbeing of humans. Water pollution, according to the World Health Organization, is a change in the composition of water caused by human activities, either directly or indirectly.

Drinking water contaminated with viruses can cause illnesses such as hepatitis, cholera, giardiasis, typhoid, methemoglobinemia, and other complications, especially in infants and newborns who have a low immune system. It can also lead to a loss of water supply, a deteriorated surface water system, high clean-up costs, high prices for alternate water sources, and/or significant health issues. The chemical composition of groundwater is determined by a number of elements, including the frequency of precipitation, the length of time rain water stays in the root zone, and so on. As a result, groundwater contamination is almost entirely due to human activities, particularly in locations where population density is high and land use is intensive. The identification of aquifer recharge zones is an important part of mitigating groundwater pollution, and in such area the protection is very vital.

The motivation for this study was bored out of the need to assist the inhabitant of Ibulesoro in the area of groundwater exploration and exploitation so as to forestall incessant drilling of abortive borehole. Many existing literatures basically centered study of this nature on one or two techniques, with may not give comprehensive results desired, even though cost also may be a major hindrance. Hence this study incorporates aquifer properties, the quality of its water content, and its vulnerability to vertical contamination to decipher the nature of the aquifer and its geochemistry.

2. Method

2.1. Study Area

Ibulesoro is a town in Ondo State, Nigeria, in the Ifedore Local Government. Araromi, Iwoye, Oju oja, Olubule, Ayetoro, and Imogun are the six quarters that make up Ibulesoro. Longitude 0732900 – 0733900mE and Latitude 0809400 – 0809000mN are the coordinates for this location. It is around 80 km^2 in size. The location can be reached via the Akure – Ilesha Highway and the Akure – Aule Road (Fig. 2). The people's primary occupation is farming. The landscape is steep and moderate sloping, with topographical elevations ranging from 350 to 388 meters (Fig. 2), and the area is bordered by isolated hills/ridges of various geological formations. The tropical rainforest climate which the fall within, is divided into two seasons: wet (March – October) and dry (November – February). When it comes to rainfall frequency and severity, the months of June through September are high, thus leading to high soil saturation, soil erosion and flooding. July and September are the wettest months in the area, with periodic, strong downpours. During the downpour, rainfall of more than 42 mm can be recorded in a single day. The yearly rainfall is 1500 mm, and the average temperature ranges from 18 to 33 degrees Celsius [45]. Because sunshine duration/intensity is short (2.7 to 2.9 hours per day) and evaporation is minimal (between 3 and 4 mm per day) from June to September, relative humidity can reach 90 percent [45].

2.2. Geology and Hydrogeology

The study region is defined by crystalline rock from southern Nigeria's Precambrian basement complex. Migmatite-gneiss, gneiss, biotite gneiss, biotite granite, and granite are the geological units found in the area. The most common is migmatite gneiss, while biotite granite is porphyritic and medium to coarse grained. Granites are found in low-lying outcrops as intrusive. Fractures, veins (pegmatitic, quartzo-feldspathic, and quartz veins), joints, and faults (Figures 3 & 4) can be found with NW-SE and NE-SW structural trends. The rock units are outcropped in various areas. Hydrogeologically, groundwater accumulation is a function of weathering, overburden thickness, degree and nature of fracturing rocks, infiltration/percolation, and aquifer hydraulic capabilities. Secondary porosity and permeability of basement bedrock generated by cracks, joints, faults, and sheared basement bedrock are responsible for such groundwater production. Groundwater yield can also be enhanced by the presence of pegmatitic, quartz, and quartzo-feldspathic veins. The weathered layer and unconfined/confined fractured basement are the area's primary water-bearing units. The aquifer's transmissivity and potentiometric surface, the amount of precipitation that is not lost through evapotranspiration and runoff; the coefficient of permeability of surficial deposits and other strata in the aquifer's recharge area; are some of the factors which determines the volume of recharged water capable of moving downward to the aquifer.

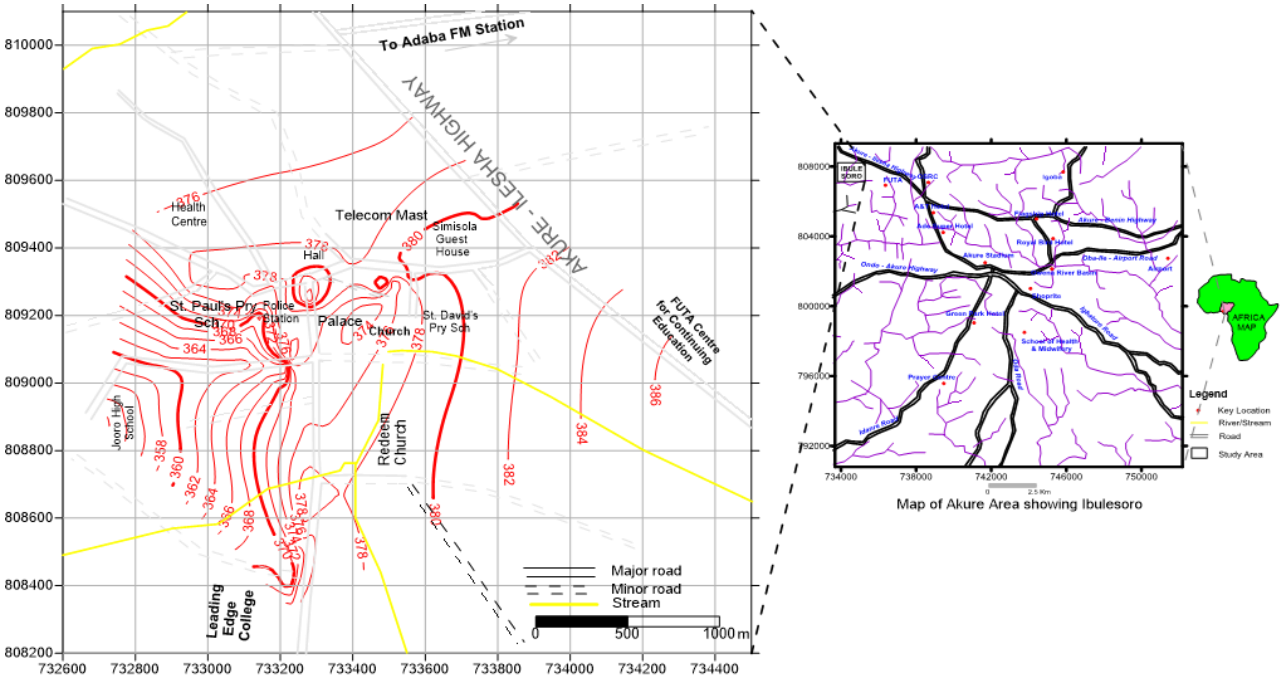

Figure 2. Location map and the topographical variation across the study area

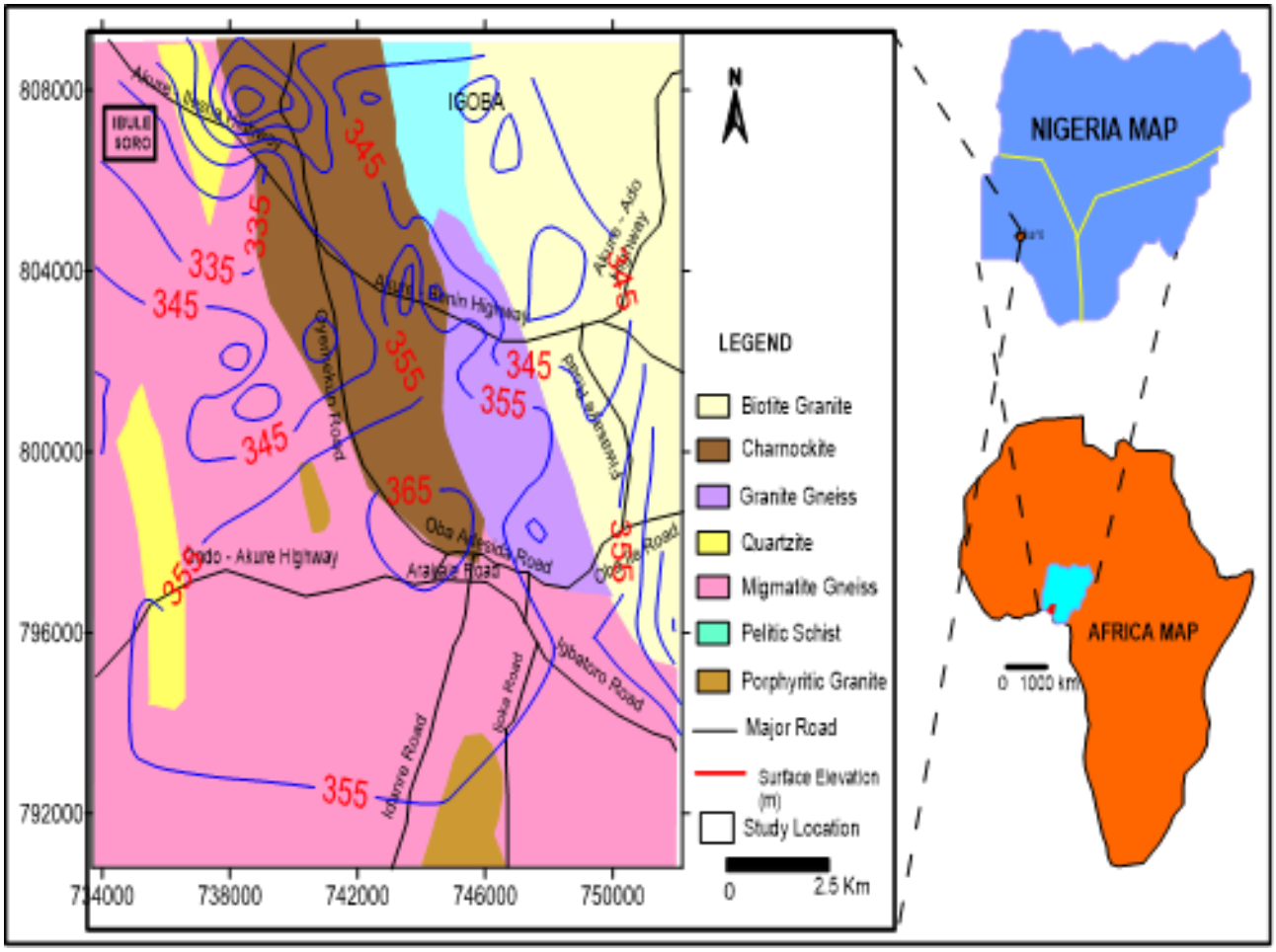

Figure 3. Geological Map of Akure with overlay of elevation variation (modified after [44, 46])

Figure 4. Field Pictures of Geologic units observed varying from migmatite, granite gneiss, granite, biotite gneiss/granite from boulders, low lying, and ridges. The Gneiss shows conspicuous banding; and also, presence of veins especially on migmatite

The study methods employed electrical resistivity, borehole drilling, water quality analysis, and hydrogeological measurements. The data acquisition map is shown in Figure 5. The electrical resistivity utilized the vertical electrical sounding method (VES) data using Schlumberger array using Telford et al. [14] outlined methodology/procedure [16, 44], with current spacing of 100 m. The data collected were processed and interpreted using combination of curve matching and computer iterative modeling [47]. Several hydrogeophysical maps which include depth to aquifer, aquifer thickness, overburden, hydraulic and transmissivity maps were generated. The VES stations were chosen based on geology, topography, the presence of existing water wells/boreholes, and accessibility. The nature and thickness of the overburden, fracture contrast, reflection coefficient, formation factor, traverse resistance, hydraulic conductivity, transmissivity, longitudinal conductance, and AVI were all combined to produce a groundwater potential map for the area. Equation (4) was used to get the reflection coefficient.

$$r = \frac{(\rho_n - \rho)(n-1)}{\rho_n + \rho(n-1)} \quad (4)$$

Where r is reflection coefficient, ρ_n is the layer resistivity of the nth layer and $\rho_{(n-1)}$ is the layer resistivity overlying the nth layer. The fracture contrast was calculated using equation (5).

$$F_c = \frac{\rho_n}{\rho_n - 1} \quad (5)$$

The traverse resistance was calculated using equation (6).

$$T = \sum_{i=1}^{n} \rho_i h_i \quad (6)$$

where T is traverse resistance, ρ and h are resistivity and thickness of the nth layer respectively. The longitudinal conductance and aquifer vulnerability index (AVI) were used to measure the susceptibility or protective capability of the vadose zone/overburden material to pollution/contamination. These approaches combine or reflect texture, structure, thickness, level of organic carbon, mineral composition of the clay, permeability, geology, and other hydrogeologic factors intrinsic properties [16]. The longitudinal unit conductance (equation 7) was used to predict the water's contamination susceptibility using geoelectrical characteristics [48-49].

$$LC = \sum_{i}^{n} \frac{h_i}{\rho_i} \quad (7)$$

where LC is longitudinal conductance, h_i and ρ_i are the thickness and resistivity of nth layer respectively.

The AVI method measures hydraulic resistance (c) to vertical flow [20] using the thickness of the water bearing units and hydraulic conductivity as shown in equation (8).

$$c = \sum d\_i/K\_i \quad (8)$$

for layers 1 to i. The interpretation of "c" was done using Table 1. In addition, data was gathered from four existing boreholes, and twenty five (25) water wells. The static water level was calculated using these wells. VES was located or conducted in fifteen (15) of these well locations for the purpose of correlation.

Table 1. Relationship of hydraulic resistance (c) and Aquifer Vulnerability index

Hydraulic resistance (c)	Log (c)	Vulnerability
0 – 10	<1	Extremely high
10 – 100	1 – 2	High
100 – 1,000	2 – 3	Moderate
1,000 – 10,000	3 – 4	Low
>10,000	>4	Extremely low

Pumping tests were used to assess the hydraulic properties of the wells and boreholes, as this is one of the most effective approaches to determine or estimate the physical qualities of water bearing layers [20]. The ultimate goal is to find a suitable drilling point/location with the lowest pumping cost, pumping water free of sand and silt, a well/borehole with the lowest operating and maintenance costs, and a well/borehole with a long and economical lifetime. The ease with which liquid flows through a medium is measured in hydraulic conductivity (K). Unlike intrinsic conductivity, which characterizes the water transmitting capabilities of a porous media, it incorporates both medium and flow attributes (equation 9):

$$T = Kh \quad (9)$$

where T is transmissivity, K is hydraulic conductivity, and h is thickness of the water bearing unit. The formation factor (Fm) was computed for each of the geological units in the area.

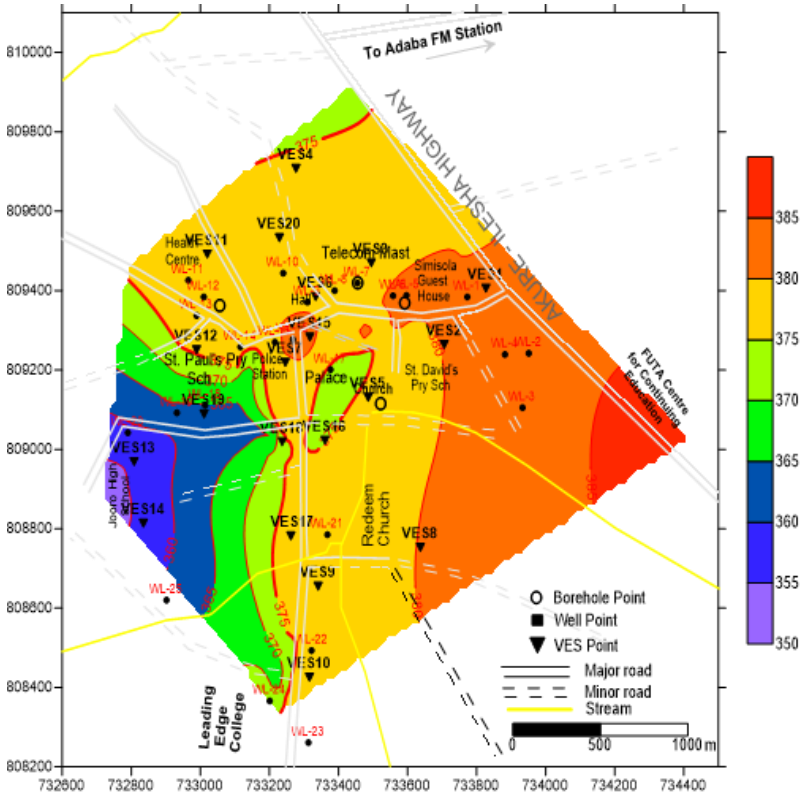

Figure 5. Data Acquisition map showing the locations of the VES, collected water samples, drilled borehole, and hydrogeological measurements from 25 wells

The Fm considers all of the characteristics of the material that affect electrical current flow, such as diagenetic cementation, pore shape, and porosity [7]. In this study, the obtained Fm was associated (r^2) with hydraulic conductivity. The Formation factor was calculated using Equation (10). A conductivity meter was used to measure the conductivity (in mhos) of the water at the site and convert it to ohm-m. The hydraulic conductivity of aquifers with no well/borehole data was calculated using a hydraulic conductivity and formation factor regression equation that was generated. Since a regression expression was built between the two; for each of the formations, transmissivity was estimated as well for all the VES stations.

$$Fm = \frac{average\ aquifer\ water\ \ resistivity}{resistivity\ of\ water\ at\ site} \quad (10)$$

The easiest way to determine aquifer parameters like K and T is to use data from well pumping tests. These characteristics play a role in regulating the water moving naturally through an aquifer as well as the resistance to fluid extraction. A global positioning system was used to assess SWL from twenty-five open wells. The GPS was used to determine the elevation of the well locations in relation to sea level, while the well's meter rule was lowered into the various wells until it reached the bottom, at which point the measurement was taken at the depth to the well's bottom. Hydraulic head and water column thickness are two more metrics taken. The measurement was taken twice, while the average values were recorded.

Before the rainy season began, ten groundwater samples were obtained at random with polythene bottles to ensure that effluents from runoff did not affect the quality of open wells, less than 10 meters deep. Pre-cleaning of the polythene bottles included Using non-ionic detergents, water, and then de-ionized water for the final rinse [50]. The water wells' locations were geo-referenced accordingly. Standard methodologies and techniques were used to analyze physical, chemical, and biological properties in samples delivered to the lab. At the time of collection, the samples' color, smell, turbidity, taste, appearance, pH, and total dissolved solids (TDS) were measured using a digital multimeter along with the samples' temperature using a mercury-in-glass thermometer. The electrical conductivity of the samples was measured using a digital conductivity meter. The total alkalinity was calculated using the titrimetric method (TA). Total Hardness was determined using EDTA (Ethylene Diamine Tetra Acetic Acid) as a titrant in a PH-10 buffer solution. The content of chlorine was determined using Mohr's method. Calcium, magnesium, potassium, and sodium were determined using a visible spectrophotometer; sulphate, bicarbonate, and nitrate were determined using the calometric method (digital titration). All of the testing were carried out according to APHA guidelines [51]. The ionic balance error (IBE) was calculated using equation (11), and the analytical precision for ion measurements (in meq/l) was determined to be +7%. The value is often within the acceptable range of 10%. As a result, the information can be used for any purpose to interpret the quality of groundwater (drinking purpose and irrigation).

$$IBE = \frac{(TCC+TCA)}{TCC-TCA} \times 100 \quad (11)$$

where, TCC = total concentration of cations; TCA = total concentration of anions

The biological parameters that were tested were total coliform and E. coli. The American Public Health Association's [51] procedures for collecting and analyzing water samples were rigorously followed. A Piper diagram was used to represent and compare the water quality analyses in the research area. Data was subjected to statistical analysis using correlation and principal component analysis to better understand the nature of groundwater and the correlations between recorded characteristics (PCA).

One of the most successful methods for expressing information about water quality to concerned citizens and policymakers is the water quality index. It has become a critical metric for assessing and managing groundwater around the world, procedure developed by Sakati and Sarma [52] was adopted in this study, by assignment of weight (w_1) to each parameter measured in the water samples according to their relative importance in the overall quality of water for drinking purpose. In this study, a maximum weight of five (5) was assigned to NO_3^-, K^+, Fe^{2+}, TDS, Cl^-, E-Coli, and total coliform; four (4) to pH, EC and Mn^+; three (3) was assigned to Ca^{2+}, Mg^{2+}, HCO_3^-, and SO_4^{2-}; while Na^+, turbidity, and total hardness (TH) assigned a weight of two (2); temperature and Alkalinity assigned a weight of one (1). Equations (12)-(14) were used in calculating WQI for the samples.

$$W_i = \frac{w_i}{\sum_{i=1}^{n} w_i} \quad (12)$$

where, Wi is the relative weight, wi is the weight of each parameter and n is the number of parameters.

$$q_i = \frac{C_i}{S_i} \times 100 \quad (13)$$

where, qi is the quality rating, Ci is the concentration of each chemical parameter in each water sample in milligrams per liter, Si is the World Health Organization water standard for each chemical parameter in milligrams per liter.

$$WQI = \sum_{i=1}^{n} SL_i \quad (14)$$

where SLi is the product of Wi and qi. According to Rao and Nageswararao [41], the suitability of WQI values for human consumption was applied in this investigation, as shown in Table 2.

Table 2. Water Quality Indices Rating

WQI values	Rating
0-25	Excellent
26-50	Good
51-75	Bad
76-100	Very Bad
100 & above	Unfit

Permeability Index (PI), Magnesium ratio (MR), Kelly ratio (KR), percent Na, salinity hazard utilizing EC values, sodium absorption ratio (SAR), and residual sodium carbonate (RSC) in meq/l were calculated for irrigation purposes using equations (15)-(20), and the results were rated with standard values [23,53].

$$SAR = \frac{Na^+}{\sqrt{\frac{Ca^{2+} + Mg^{2+}}{2}}} \quad (15)$$

$$\%Na^+ = \frac{(Na^+ + K^+)}{(Ca^{2+} + Mg^{2+} + Na^+ + K^+)} \times 100 \quad (16)$$

$$PI = \frac{Na^+ + \sqrt{HCO_3^-}}{Ca^{2+} + Mg^{2+} + Na^+} \times 100 \quad (17)$$

$$RSC = (HCO_3^- + CO_3^{2-}) - (Ca^{2+} + Mg^{2+}) \quad (18)$$

$$MR = \frac{Mg^{2+}}{Ca^{2+} + Mg^{2+}} \quad (19)$$

$$KR = \frac{Na^+}{Ca^{2+} + Mg^{2+}} \quad (20)$$

3. Results

3.1. Electrical resistivity

Table 3 summarizes the geoelectric characteristics and inferred lithologies, whereas Figure 6 shows the different types of curves. As is typical of the subterranean complex terrain, the individualities of the geoelectric curves differed substantially. They range from three layer A-type (15%), H-type (10%), and K-type (5%), to four layer HA-type (10%), KH-type (40%), HK-type (15%), and five layer HKH-type (5%). The KH-type is the most common, with the four layer curve types accounting for 65 percent of all curve types. This indicates the degree of heterogeneity within weathered profile and fracturing of the basement rocks [10].

Three to five geologic sequences were discovered by the geoelectric interpretations. geologic sequence, as follows: topsoil (25–222 ohm-m; 89 ohm-m avg.), thicknesses (0.5 – 1.2 m; 0.9 m avg.), composed of clay, and sandy clay. Below the topsoil is a layer composed of clay/sandy clay/clay sand (33-320 ohm-m; 150 ohm-m avg.), thicknesses (2.2 – 7.5 m; 3.9 m avg.); the weathered layer, which is composed of clay/sandy clay and clayey sand (29–365 ohm-m; 96 ohm-m avg.), thicknesses (2.3 – 17.5 m; 9.1 m avg.); the partly weathered/fractured layer (25–412 ohm-m; 250 avg.), thicknesses (6.1 – 11.5 m; 8.6 m avg.); and the fresh basement (221–9540 ohm-m; 1861 ohm-m avg.). The depth to the basement rocks ranged from 5.7 to 32.5 m (16.1 m avg.). The water bearing units is basically found in the weathered layer, and confined/unconfined fractured basement which were only delineated in few places.

The spatial distribution of the weathered layer's resistivity and thickness map (Fig. 7a) revealed a prominent resistivity in the 80–200 ohm-m range, corresponding to a clay/sandy clay water bearing unit, whereas resistivity range of 150 - 300 ohm-m (sandy clay/clay sand) was observed in the extreme northern part. The isopach map of the weathered layer (Fig. 7a) revealed overlapping values across the study area in the range of 6 – 15 m. On the southwestern flank, however, noticeable low thicknesses less than 10 m are observed. The overburden thickness of all VES curves ranges from 5.7 to 32.5 m (Fig. 7b and Table 4), with an average of 16.1 m. The spatial distribution of the overburden thickness (Fig. 7c) decreases northward; while higher values greater than 14 m are seen in the central – southern part. In reality, the presence of a thick aquiferous geologic unit does not necessarily suggest a large water yield, as important characteristics like resistivity, hydraulic gradient, sorption, hydraulic conductivity, transmissivity, and so on still play a role [6].

Table 4 shows that the traverse resistance (TR) ranges from 161.1 to 21896.1 ohm-m^2 (avg. 2202.9 ohm-m^2). Aquifer transmissivity and traverse resistance can be correlated. Transmissivity increases as the TR increases. The average value of 2202.9 ohm-m^2 is less than 5000 ohm-m^2 expected of productive aquifer with high safe yield and transmissivity. The fracture coefficient (Fc) ranged from 0.15 – 265, with an average of 32.70 (Table 4). A good water bearing unit must be able to possess low fracture contrast/coefficient in the range of 0 – 20. Consequently, the groundwater potential in the study area on the basis of Fc is low. The reflection coefficient (Rc) is also linked to groundwater yield, as a low Rc indicates a high-density water-filled fracture with a high yield/potential. Table 4 shows the Rc values obtained for this investigation, which vary from -0.32 to 0.99. (0.65 avg.). Lower Rc favours availability of groundwater at reasonable economic supply. The groundwater potential appears to be low based on Table 5 rating, using Rc and overburden thickness.

3.2 Hydraulics

The K and T values for all the VES stations were estimated from the relationship of hydraulic conductivity (x-axis) and formation factor (y-axis) and obtained from twelve wells which were dug besides the VES locations. The relationship established is $y = 0.239e^{0.0519x}$ with correlation coefficient of 0.0961. The hydraulic conductivity of the water bearing units vary from 0.22 to 1.22 m/d and an average of 0.52 m/d; the transmissivity ranges from 1.08 to 18.18 m^2/d and an average of 5.78 m^2/d (Table 4).

Using Tables 6 and 7, the geological units fall within soil of clay-sand mixture depicting semi-permeable soil material. The spatial distribution of K and T (Fig. 7 c,d) shows that transmissivity is higher in the south with relatively high K-values, while the central part is moderate. Hence the hydrogeological parameters increase southwardly. The information obtained from the wells are presented in Table 8. The static water level which is invariably the thickness of the vadose water zone, varies from 3.9 – 7.9 m with an average of 5.68 m. The total depth of the wells varies from 5.8 m to 10.5 m and an average depth of 7.9 m, with water column of 1.3

– 3.7 m (2.2 m avg.). The obtained K and T ranged from 0.13 – 0.84 m/d (0.41 m/d avg.) and 0.77 – 16.9 m^2/d (6.66 m^2/d avg.) respectively. These values are very close to values estimated for all the VES stations. The measured pore water resistivity varied from 34.84 – 53.48 ohm-m (43.12 ohm-m avg.), while groundwater formation factor (Fm) ranges from 0.59 to 11.33, with average value of 4.02.

Table 3. Summary of the VES Results obtained in the study area

Location		Elevation	VES	RESISTIVITY (Ohm-meter)					THICKNESS (m)				DEPTH (m)				Curve
East	North	(m)	NO.	ρ_1	ρ_2	ρ_3	ρ_4	ρ_5	h_1	h_2	h_3	h_4	d_1	d_2	d_3	d_4	Type
733827	809406	381	1	78	365	1032			0.9	17.5			0.9	18.4			A
733706	809264	380	2	71	45	815	3281		1.1	4.9	26.5		1.1	6.0	32.5		HA
733495	809470	378	3	69	221	1480			0.8	4.9			0.8	5.7			A
733277	809708	375	4	98	254	69	2132		1.0	3.2	15.5		1.0	4.2	19.7		KH
733486	809131	375	5	101	189	68	2248		0.8	7.5	13.8		0.8	8.3	22.1		KH
733334	809385	378	6	78	155	36	9540		1.2	3.5	14.9		1.2	4.7	19.6		KH
733246	809219	378	7	87	122	59	1099		1.0	4.2	12.2		1.0	5.2	17.4		KH
733637	808753	380	8	126	320	98	1247		0.9	2.6	13.3		0.9	3.5	16.8		KH
733341	808655	378	9	56	147	658			1.0	15.5			1.0	16.5			H
733316	808426	376	10	25	211	98	2003		0.8	2.2	8.9		0.8	3.0	11.9		KH
733020	809492	376	11	84	155	369			0.7	5.9			0.7	6.6			K
732989	809251	376	12	63	29	356	221		0.9	3.6	11.5		0.9	4.5	16.0		HK
732808	808969	356	13	45	148	654			1.2	6.8			1.2	8.0			A
732835	808814	356	14	56	101	29	2332		1.2	6.1	9.2		1.2	7.3	16.5		KH
733317	809283	381	15	45	230	63	1983		0.6	2.8	7.1		0.6	3.4	10.5		KH
733361	809023	374	16	73	40.4	286	3262		0.8	3.9	12.5		0.8	4.8	17.2		HA
733262	808782	376	17	89	33	159	25	1425	0.5	2.7	4.9	6.1	0.5	3.2	8.1	14.2	HKH
733237	809019	373	18	92	47	661	341		1.1	2.3	5.3	6.8	1.1	3.4	8.7	15.5	HK
733011	809089	363	19	158	99	752	412		1.0	4.5	7.9	9.9	1.0	5.5	13.4	23.3	HK
733229	809533	377	20	222	79	1498			0.8	13.5			0.8	14.3			H

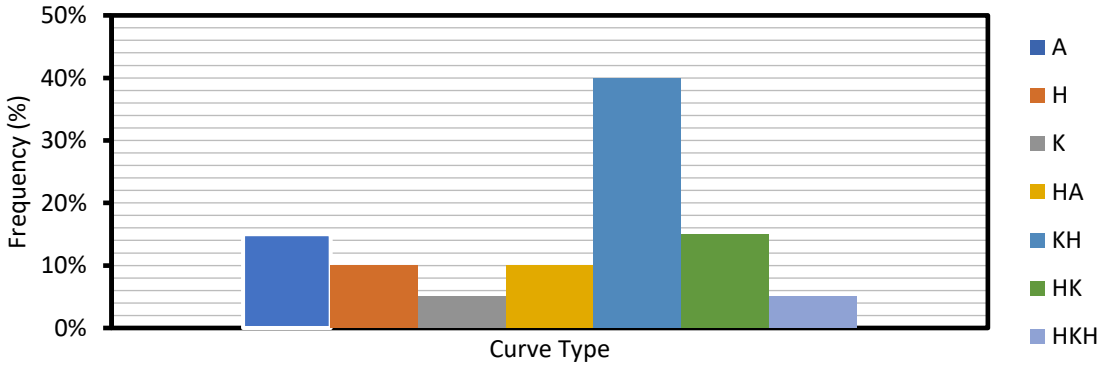

Figure 6. Curve types obtained from ves interpretation

Table 4. Summary of geoelectrical/hydraulics characteristics, vulnerability and groundwater potential index values of the Water Bearing units in the Study

VES No.	Overburden (m)	TR (ohm-m^2)	FC	RC	K (m/d)	T (m^2/d)	LC (ohm-m)$^{-1}$	Log (c)	GWPIV	GWPIV Rating
1	18.4	6457.7	2.83	0.48	0.36	6.25	0.0595	0.40	171	Moderate
2	32.5	21896.1	4.03	0.60	0.25	6.63	0.1569	0.64	158	Moderate
3	5.7	1138.1	6.70	0.74	0.22	1.08	0.0338	0.56	128	Low
4	19.7	910.8	30.90	0.94	0.26	4.03	0.0228	1.21	127	Low
5	22.1	1498.3	33.06	0.94	0.29	4.06	0.0476	1.46	127	Low
6	19.6	636.1	265.00	0.99	1.22	18.18	0.0380	0.59	134	Low
7	17.4	599.4	18.63	0.89	0.29	3.59	0.0459	1.25	131	Low
8	16.8	945.4	12.73	0.85	0.60	7.98	0.0153	0.77	131	Low
9	16.5	2334.5	4.48	0.64	0.67	10.39	0.1233	0.17	148	Low
10	11.9	1356.4	20.44	0.91	0.65	5.79	0.1332	0.09	112	Low
11	6.6	973.3	2.38	0.41	0.59	3.48	0.0464	0.07	126	Low
12	16	161.1	0.62	-0.23	0.63	7.25	0.1384	0.15	133	Low
13	8	1060.4	4.42	0.63	0.61	4.15	0.0726	0.29	122	Low
14	16.5	683.3	80.41	0.98	0.32	2.97	0.0818	1.36	117	Low
15	10.5	1118.3	31.48	0.94	0.60	7.50	0.1382	0.75	112	Low
16	17.2	216.0	11.41	0.84	0.63	3.84	0.1075	0.88	125	Low
17	14.2	912.7	0.15	0.97	0.64	4.35	0.1183	-0.11	116	Low
18	15.5	209.3	0.52	-0.32	0.29	2.92	0.0609	0.58	133	Low
19	23.3	603.5	0.55	-0.29	0.60	2.70	0.0518	0.22	133	Low
20	14.3	347.8	123.23	0.98	0.63	8.51	0.1433	0.10	114	Low

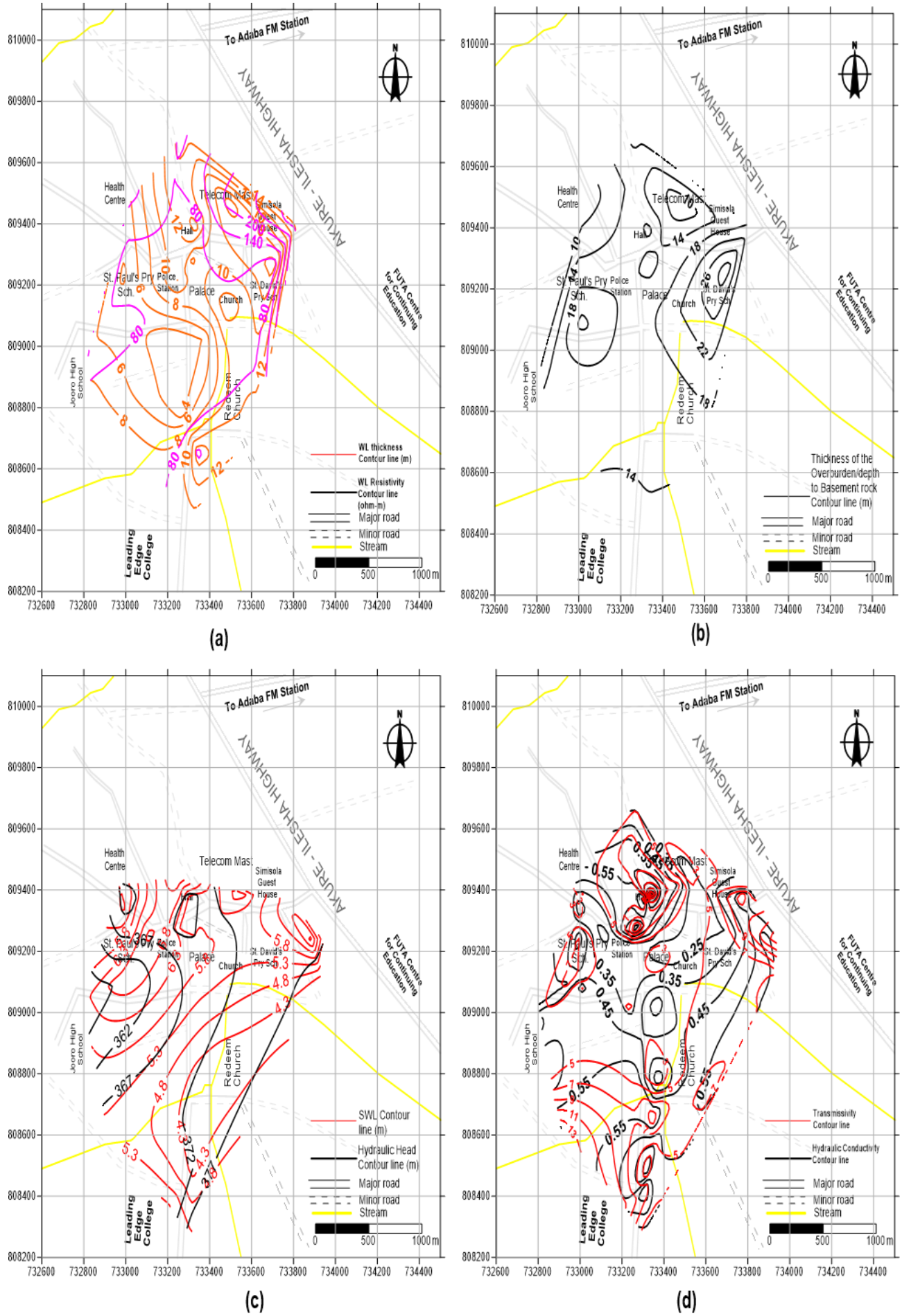

Figure 7. Spatial Distribution of (a) weathered layer thickness and resistivity (b) overburden thickness (c) static water level and hydraulic head (d) hydraulic conductivity and transmissivity

Table 5. Longitudinal unit conductance, overburden thickness, and reflection coefficient with corresponding protective rating

Total Longitudinal unit Conductance (mhos)	Rating of overburden's aquifer protective capacity	Overburden Thickness (m)	Reflection Coefficient	Groundwater Yield
<0.10	Poor	>15	>0.5	High
0.1 – 0.49	Weak	>15	<0.5	Medium
0.5 – 0.99	Moderate	<15	>0.5	Low
1.0 - 4.99	Good	<15	<0.5	Very Low
5.0 – 10.0	Very good			
>10.0	Excellent			

Table 6. Order of magnitude of K for different kinds of rock [54]

Geological Classification Unconsolidated Materials	K (m/d)
Clay	10^{-8} - 10^{-2}
Fine sand	1 - 5
Medium sand	5 - 2×10^{1}
Coarse sand	2×10^{1} - 10^{2}
Gravel	10^{2} - 10^{3}
Sand and gravel mixes	5 - 10^{2}
Clay, sand, gravel mixes	10^{-3} - 10^{-1}
Rock	
Sandstone	10^{-3} - 1
Carbonate rock with secondary porosity	10^{-2} – 1
Shale	10^{-7}
Dense solid rock	$<10^{-5}$
Fractured weathered rock (Core samples)	Almost 0 - 3×10^{2}
Volcanic rock	Almost 0 -10^{3}

Table 7. Classification of Water Bearing Geological Units based on Coefficient of Permeability [54]

Class	K (m/d)	Examples
Extremely permeable	>10	Coarse sandstone, limestone and fissured crystalline rocks, pebbles, gravels
Semi-permeable	10-0.1	Fine grained sands, loams, slightly jointed crystalline rocks
Impermeable	<0.1	Clays, marls, compact igneous rocks

High formation factor corresponds to productive aquifer with good water yield. Therefore, based on this, the groundwater yield/potential in the area is low.

3.3 Borehole logging

The nature of parent rock, depth, amount and pattern of weathering, the sand/clay ratio, and the degree of fracturing, fissuring, and jointing all influence the occurrence of groundwater. Figure 8 shows the columnar section of the four drilled boreholes (BH-1 - BH-4) in the area. The column depicts five geological units based on physical observation/inspection of cuttings during drilling. The sections revealed that DBH-1 comprises four units: clay-sand mixture, sandy clay, fractured basement, fresh basement (gneiss), delineated at depth boundaries of 2.5 m, 25 m and 32.5 m respectively.

BH-2 has four unit, consisting of clay-sand mixture, clayey sand grading to clayey soil, sandy clay, fresh basement (granite), with lithological depth boundaries of 1.5 m, 16 m, and 39.9 m respectively. BH-3 consists of clayey sand, sandy clay, clay sand mixture, fractured basement, and fresh basement (migmatite gneiss) corresponding to geologic depth boundaries of 3 m, 6 m, 24 m, and 30 m. BH-4 is characterized by alternation of clay – sand mixture, clayey sand, clay sand grading stiffly to clayey soil, sandy clay, clay sand grading stiffly to clayey soil, sandy clay, and fresh basement (which is granitic); at lithological boundaries of 2 m, 8 m, 15 m, 32 m, and 40 m depth respectively. It was observed from the result of the drilling activity that most of productive boreholes were not drilled beyond the depth range of 30 – 35 m; therefore, this might be the reason why BH-2 and BH-4 failed and characterized with low yield. It was also observed that boreholes drilled on migmatite/migmatite gneiss, and gneiss tend to be productive than granite, even though the fractured/partly weathered layer proved to be the difference between this geological units in the study area. Consequently, the combined weathered zone and fractured basement (unconfined aquifer) is the best groundwater configuration for productive exploitation and development in the area as revealed by the geologic sections (Fig. 8).

3.4 Vulnerability Assessment

The vulnerability of the water bearing units were assessed by AVI and LC as shown in Table 4. The calculated longitudinal unit conductance values (in mhos) of water bearing units using resistivity parameters ranged from 0.0153 to 0.1569 mhos with an average of 0.0818 mhos. Hence using Table 1, the groundwater protective capacity varies from poor – weak, while taking the average value, the protective capacity is poor. The calculated AVI values range from -0.11 – 1.46, with an average of 0.5715. Therefore, using Table 2, the groundwater in the study area is extremely vulnerable to pollution.

3.5 Groundwater Quality

The geochemistry of groundwater may have an impact on how useful aquifer systems are as water supplies. Without prior treatment, the types and concentrations of dissolved elements in an aquifer system's water determine whether the resource is suitable for drinking water, industrial uses, irrigation, livestock watering, and other uses [55-57]. Tables 9 and 10 reflect the findings of the examinations of the water

samples. The analysis's range and mean concentrations are compared to WHO [58] criteria. The usefulness of water for many uses is influenced by the earth's temperature. The groundwater's temperature ranges between 27.5 and 27.8°C, with a mean of 27.6°C. A generally moderate temperature is shown by the range of values. All of the water samples have a clear look and are tasteless, odorless, and colorless. The average turbidity of water is 9 NTU, which is higher than the WHO-recommended limit of 5 NTU and ranges from 2 to 16 NTU. This shows that the groundwater has a high suspended matter content, including clay, silt, fine organic matter particles, and similar stuff [59-61]. The pH plays a vital role to react with acidic or alkaline. It is controlled by CO_2 – CO_3^{2-} - HCO_3^- equilibrium. The combination of CO_2 with H_2O (water) forms H_2CO_3 (carbonic acid), which affects the pH of water. Based on pH, which ranges from 1 to 14, water can be categorized as acidic or alkaline. The groundwater's pH has been measured to range from 4.7 to 5.6. The water is classified as having an acidic condition according to the pH scale because H+ is more than OH- (Table 11) in the water [7, 24].

The ability of a material to carry electrical current is measured by its electrical conductivity (EC). Strong acids like Cl-, SO_4^{2-}, and NO_3^- have high conductivity compared to weak acids like HCO_3^- and CO_3^{2-}, which have low conductivity. EC ranges from 149 to 391 S/cm (avg. of 234 S/cm). The enrichment of salts in water increases with increasing EC. Using Table 12, the water can be categorized as Type I (EC less than 1500 S/cm), which is characterized by low salt enrichment, low infiltration, high runoff, and high topography. This type of water is assumed to be a recharge water. Total dissolved solids (TDS), which includes any organic matter and some water of crystallization, are a measure of the total salt concentration of dissolved ions from soils and rocks in water. The solubility and type of rocks the water has come into contact with affect the volume and makeup of dissolved solids.

Table 8. Summary of well Information, Sample locations, and measured properties

Well No.	Easting (mE)	Northing (mN)	Elevation (m)	Well Depth (m)	SWL (m)	Water Column (m)	Hydraulic Head (m)	K (m/d)	T (m^2/d)	Pore water Resistivity (Ohm-m)	Aquifer Resistivity (Ohm-m)	Formation Factor
WL-1 (VES 1)	733773	809384	381	10.2	6.6	3.6	373	0.67	12.33	47.17	365	7.74
WL-2	733951	809242	382	8.3	5.1	3.2	377	0.52	16.90	49.50	-	-
WL-3	733933	809105	383	7.7	4.0	3.7	379	0.68	3.88	40.82	-	-
WL-4	733882	809239	382	9.4	7.5	1.9	375	0.72	14.18	34.84	-	-
WL-5	733597	809388	381	6.8	5.2	1.6	376	0.22	4.86	46.73	-	-
WL-6	733558	809387	380	6.7	4.4	2.3	376	0.15	2.94	43.67	-	-
WL-7 (VES 3)	733455	809419	378	7.2	5.2	2	373	0.48	8.35	42.37	-	-
WL-8	733389	809400	377	7.1	5.8	1.3	371	0.61	10.25	37.17	-	-
WL-9 (VES 6)	733310	809371	378	6.9	5.5	1.4	373	0.23	3.80	38.91	36	0.93
WL-10 (VES 15)	733240	809444	377	10.5	7.9	2.6	369	0.58	6.90	39.06	63	1.61
WL-11 (VES 11)	732965	809426	377	7.5	4.8	2.7	372	0.47	3.10	45.05	369	8.19
WL-12	733010	809384	378	6.8	5.0	1.8	373	0.32	5.12	35.97	-	-
WL-13	732989	809337	378	6.5	4.7	1.8	373	0.15	1.20	44.05	-	-
WL-14 (VES 12)	733116	809258	376	9.3	7.5	1.8	369	0.19	3.14	38.31	221	5.77
WL-15 (VES 7)	733216	809270	378	8.6	6.6	2	371	0.66	6.93	50.51	59	1.17
WL-16	733268	809277	383	7.8	5.6	2.2	377	0.84	14.45	53.48	-	-
WL-17 (VES 5)	733377	809201	374	8.1	6.0	2.1	368	0.15	2.13	49.75	68	1.37
WL-18	733014	809111	364	9.9	7.2	2.7	357	0.43	6.67	42.37	-	-
WL-19 (VES 19)	732932	809092	364	8.4	6.9	1.5	357	0.33	7.69	36.36	412	11.33
WL-20 (VES 13)	732790	809042	358	8.3	6.1	2.2	352	0.25	3.58	50.25	148	2.95
WL-21 (VES 17)	733368	808785	377	5.8	3.9	1.9	373	0.17	1.34	42.37	25	0.59
WL-22 (VES 10)	733322	808493	376	6.7	4.1	2.6	372	0.13	0.77	37.59	98	2.61
WL-23	733313	808261	385	6.9	5.4	1.5	380	0.27	1.22	45.87	-	-
WL-24	733201	808366	373	9.5	5.9	3.6	367	0.48	9.98	38.46	-	-
WL-25	732902	808620	375	7.2	5.2	2	370	0.66	14.78	47.39	-	-

Table 9. Result obtained from the physical parameters measured/examined

Well No.	Temp (°C)	pH	TDS (mg/l)	EC (μS/cm)	Colour	Taste	Odour	App.	Turb. (NTU)
WL-1	27.6	5.40	262	391	Colourless	unobjectionable	unobjectionable	Clear	2.0
WL-4	27.7	4.79	102	149	Colourless	unobjectionable	unobjectionable	Clear	6.0
WL-8	27.8	5.56	137	204	Colourless	unobjectionable	unobjectionable	Clear	12.0
WL-10	27.8	5.20	109	162	Colourless	unobjectionable	unobjectionable	Clear	8.0
WL-12	27.5	4.80	158	236	Colourless	unobjectionable	unobjectionable	Clear	14.0
WL-17	27.6	5.18	176	262	Colourless	unobjectionable	unobjectionable	Clear	16.0
WL-19	27.6	5.45	185	242	Colourless	unobjectionable	unobjectionable	Clear	9.5
WL-20	27.5	4.68	123	198	Colourless	unobjectionable	unobjectionable	Clear	5.8
WL-21	27.5	5.50	155	205	Colourless	unobjectionable	unobjectionable	Clear	10.4
WL-22	27.8	4.95	138	290	Colourless	unobjectionable	unobjectionable	Clear	8.8

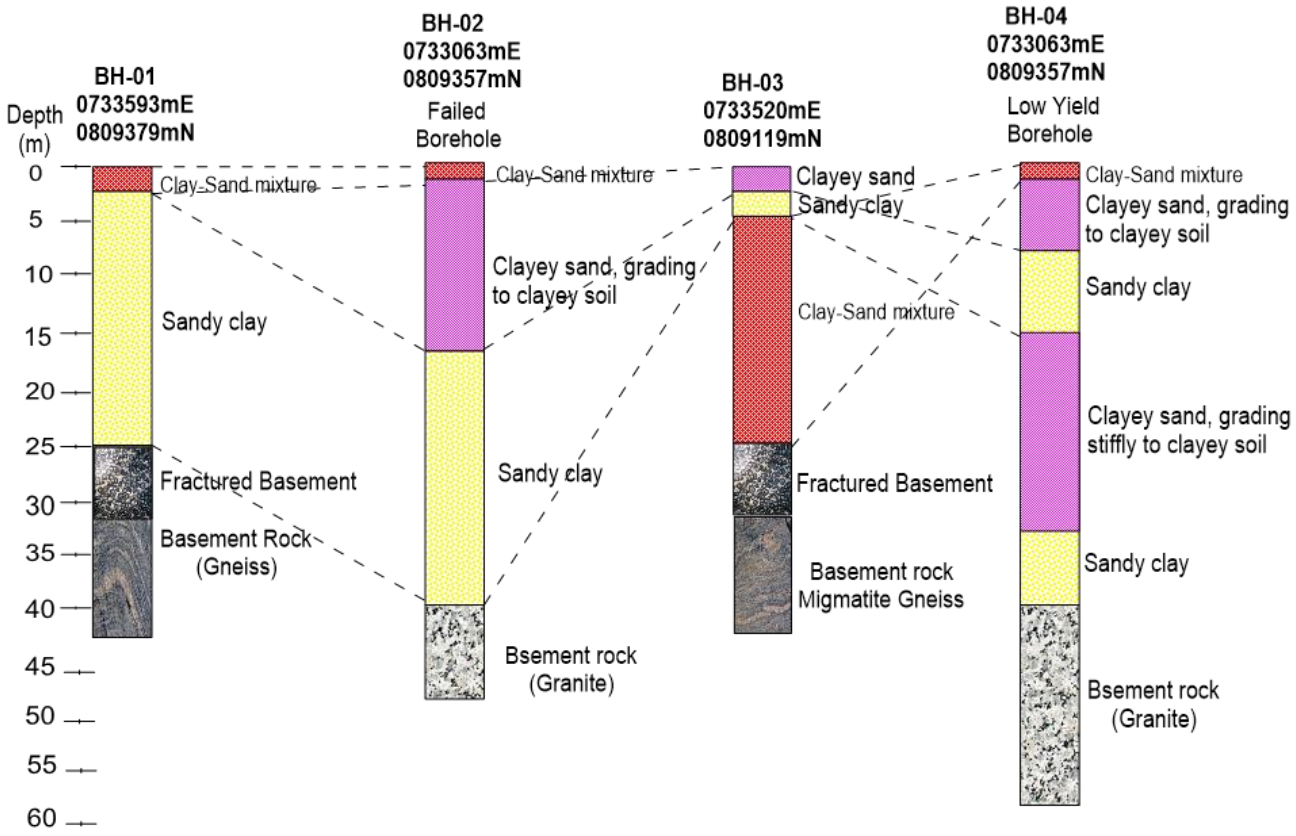

Figure 8. Columnar sections of borehole with drilling information for BH-1 to 4

Table 10. Summary of the analyzed chemical and biological parameters

Well No.	TA	TH	HCO_3^-	Ca^{2+}	Mg^{2+}	Cl^-	Na^+	K^+	SO_4^{2-}	NO_3^-	Fe	Mn	E-*Coli*	Total coliform	WQI (%)
WL-1	16	198	16.1	42.5	22.5	37.0	24.1	12.2	5.7	0.86	0.06	0.03	0	8	31
WL-4	12	64	12.7	14.4	6.23	18.0	11.0	12.5	5.2	2.44	0.08	0.02	0	6	25
WL-8	18	113	18.4	25.7	12.0	21.0	13.7	8.9	6.8	5.28	2.06	0.03	1	14	96
WL-10	9	86	9.3	16.8	29.5	15.6	10.1	7.3	8.8	1.86	0.03	0.01	0	7	27
WL-12	10	98	14.8	25.7	8.30	23.0	15.0	11.2	9.9	6.74	0.04	0.02	1	12	42
WL-17	14	176	10.0	29.7	6.33	26.0	16.9	9.8	11.2	9.36	0.06	0.02	1	18	52
WL-19	22	87	10.5	26.5	14.2	19.8	12.4	12.3	5.5	2.65	0.15	0.01	0	8	34
WL-20	17	98	14.2	17.7	19.0	24.5	13.3	9.5	11.3	1.84	0.08	0.01	1	10	32
WL-21	11	102	12.8	19.5	12.8	16.8	19.7	6.7	10.5	1.36	0.04	0.01	0	5	27
WL-22	15	122	8.6	22.6	18.3	21.9	22.8	8.3	7.6	1.11	0.09	0.02	0	6	29

Note: All units are in mg/l except the biological parameters in Cfu/100ml

High TDS is typically brought on by the impact of anthropogenic origin with regard to discharge water at topographic lows, while low TDS is typically brought on by the influence of rock-water interaction with regard to recharge water at topographic highs [24]. The value of TDS ranges from 102 mg/l to 262 mg/l (155 mg/l avg.). Therefore, using Table 13, the water is fresh with TDS less than 1000 mg/l. Total alkalinity is a gauge of how effectively calcium carbonate can neutralize acid in water ($CaCO_3$). The TA ranges from 9 to 22 mg/l (14.4 mg/l on average). The suggested WHO acceptable threshold of 200mg/l is met by this range of results. The samples' total hardness (TH), which ranges from 64 to 198 mg/l (114 mg/l on average), varies greatly. Scale develops in pipes, water heaters, and boilers due to hard water. The amount of soap lather increases with TH. The study area's water is classified as either soft or hard according to TH, as shown in Table 14. However, the water samples' TH and TA (average readings) both fall within the 400 mg/l and 200 mg/l, respectively, WHO-recommended permitted limits.

Table 11. Classification of pH [24]

pH Range	Type	Dominance of ions
1 – 7	Acid	H^+ is more than OH^-
7	Neutral	Equal amounts of H^+ and OH^-
7 - 14	Basic	OH^- is more than H^+

Table 12. Classification of EC [24]

EC Range ($\mu S/cm$)	Type	Enrichment of salts	Topography	Runoff	Infiltration	Water type
<1,500	I	Low	High	High	Low	Recharge water
1,500 – 3,000	II	Medium	Moderate	Medium	Medium	-
>3000	III	High	Low	Low	High	Discharge water

Table 13. Classification of TDS [7]

TDS range (mg/l)	Classification
<1,000	Fresh
1,000 to 10,000	Brackish
10,000 to 100,000	Saline
>100,000	Brine

Table 14. Classification of TH [7]

TH Range (mg/l)	Classification
<75	Soft
75-150	Moderately hard
150 – 300	Hard
>300	Very hard

The main component of most rocks is calcium (Ca^{2+}), which is typically derived from minerals like plagioclase, pyroxene, and amphiboles. Another source of calcium in groundwater is the presence of carbon dioxide in the soil zone. Ca^{2+} ranges between 14.4 and 42.5 mg/l (24.1 mg/l on average), which is still within the safe range of 75 mg/l suggested by the WHO. The groundwater's calcium content is derived from calcium feldspars found in the rocks in the research area. Basic igneous rocks, volcanic rocks, and metamorphic rocks all include magnesium (Mg^{2+}), which is generated from minerals including olivine, hornblende, serpentine, biotite, augite, and others. Magnesium in groundwater can also come from the sea, mining, and industrial waste. From 6.23 to 29.5 mg/l (14.9 mg/l), Mg^{2+} is present. This value range still falls within the permitted range of 50 mg/l. Sodium (Na^{+}) is under the WHO limit (50 mg/l) for drinking water as it ranges from 10.1 to 24.1 mg/l (15.9 mg/l on average). An important source of potassium (K^{+}), which ranges between 6.7 and 12.5 mg/l (9.9 mg/l on average), is found in orthoclase feldspar, nepheline, leucite, and biotite. Other sources of potassium include chemical fertilizers. K^{+}'s generally lower content may be caused by clay minerals absorbing it. As a result, the K^{+} for drinking water is within the WHO limit (75 mg/l). It ranges from 8.6 to 18.4 mg/l (12.7 mg/l on average) of bicarbonate (HCO_3^{-}). This value range is within the permissible range of the WHO guideline of 500 mg/l. The principal source of HCO_3^{-} in the groundwater is probably soil CO_2. Organic material breakdown also releases carbon dioxide for solution. Sulphate (SO_4^{2-}) levels in the examined water samples range from 5.2 to 11.3 mg/l (8.3 mg/l on average). The reported mean value complies with the 100 mg/l WHO standard for drinking water. Within the permitted limit of 250 mg/l, the chloride (Cl^{-}) is dissolved from the rocks and soils in the research region, with values ranging from 15.6 to 37 mg/l (22.4 mg/l on average). The water samples have nitrate (NO_3^{-}) concentrations ranging from 0.86 mg/l to 9.36 mg/l (3.4 mg/l). Nitrate is a compound that is produced when organic matter decomposes and is found in sewage, nitrate fertilizers, and soil. Since the NO_3^{-} level is less than 10 mg/l, it is most likely coming from suspected nitrate fertilizers as well as soil nitrate. However, the outcomes are in line with the WHO's advice.

Manganese and iron heavy metal concentrations in the water were 0.01 to 0.03 mg/l (av. 0.018 mg/l average) and 0.03 to 2.06 mg/l (avg. 0.269 mg/l average), respectively. These cation and heavy metal values are extremely low and fall under the WHO standards of 0.1 mg/l and 0.3 mg/l, respectively. The biological quality test revealed an E. coli concentration of 0 to 1 CFU/100 ml and a total bacterial count of 5 to 18 (9 avg.). These average values are below the stipulated limits of 3 Cfu/100 ml for E. coli and 10 Cfu/100 ml for total coliform, respectively. Although the total bacteria count is high. The trilinear diagram of the water samples, shown in Figure 9, is a useful tool for separating information for a critical analysis with regard to the sources of dissolved ions in water and changes in water character [62].

The majority of the water in the study area falls into zone 4 (Fig. 9b), which is classified as "strong acids exceeded weak acids," and no cation-anion pair (Ca-Mg-Cl water type) exceeds 50%. However, only a small percentage of samples (less than 20%) are of non-carbonate hardness (secondary alkalinity) exceeds 50%. (Ca-Cl water type). For the purpose of understanding the mechanisms that control the groundwater chemistry with respect to atmospheric precipitation (rainfall), rock-water interaction, and evaporation, Gibb's diagrams were used to relate the ratios of the cations ($Na^{+} + K^{+}$: $Na^{+} + K^{+} + Ca^{2+}$) and anions (Cl^{-}: $Cl^{-} + HCO_3^{-}$) that are plotted against TDS. From Figure 10, the chemistry of the water falls in the mixed zone, which indicates contribution from soil/rock-water interaction, precipitation, and evaporation (Fig. 10 a,b) and carbonic weathering is more active than the silicate weathering process (Fig. 10c). The calculated values of WQI vary from 25 % to 96 % (39.5 % avg.). The spatial distribution of WQI across the study area (Fig. 11) showed that southern generally part is characterized with WQI values less than 50%. This signifies that excellent/good water types characterized the south while the northern area is poor.

According to Table 15, the results of a correlation analysis using Pearson correlation show that there is a strong positive correlation between some of the chemical parameters, including Ca and TH (r = 0.87), TH and Cl (r = 0.85), TH and Na (r = 0.72), TH and Mn (r = 0.56), HCO_3 and Fe (r = 0.61), HCO_3 and Mn (r = 0.58), Ca and Cl (r = 0.87), Ca and Na (r = 0.62), Na and Cl (r = 0.62), Mn and Cl (r = 0.62) and Fe and Mn (r = 0.53). These chemical parameters had a strong positive connection, which suggests that they came from the same source. The untypical anthropogenic cause is clearly indicated by the negative positive association between Mg and NO_3 (r = -0.64), SO_4 and K (r = -0.57), and Mg and SO_4 in general.

Groundwater data are subjected to principal component (PC) analysis in order to better understand

the correlations between them and the likely sources of significant ions. The data set underwent an analysis of five components (Table 16). With an eigenvalue of 3.67, the principal component 1 (PC-1) explains 31% of the groundwater variance overall. TH, Ca, Cl, Na, and Mn are some of the parameters that are heavily and positively loaded on this factor. This relationship demonstrated that the precipitation of all these variables in the water samples is due to a single source.

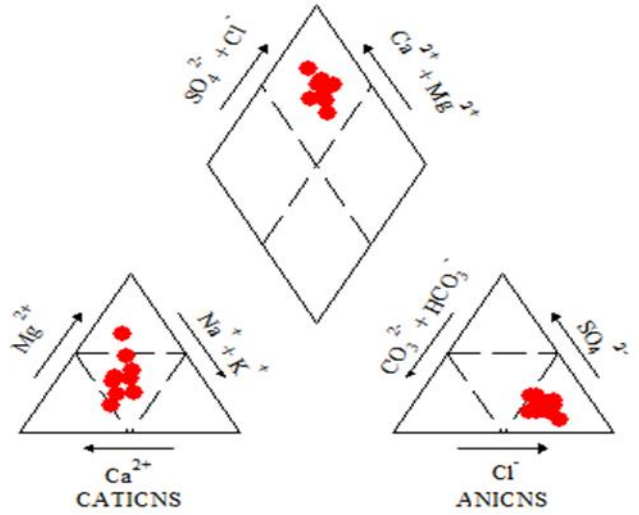

(a)

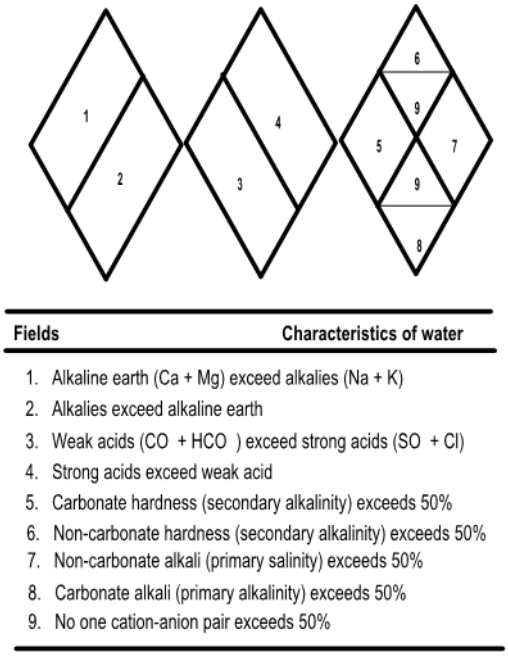

(b)

Figure 9. (a) Piper's Trilinear Diagram for Water Samples (b) showing a predominant Zone 4 Water Type

Mineral dissolution, weathering, and anthropogenic pollution have all been assigned to this component. The PC-2's eigenvalue is 2.08, which represents 17% of the overall variance. The following parameters—HCO_3, Fe, and Mg—are heavily and favorably weighted on this component. This component might be caused by precipitation or mineral dissolution as a result of the interaction between rocks and water. The eigenvalue of PC-3 is 1.89, accounting for 16% of the overall variance. Because to the deterioration of organic materials and anthropogenic contamination, this component is heavily and favorably loaded with NO3.

The PC-4's eigenvalue is 2.16, and its overall variance is 18%. The two main factors that are heavily and favorably coupled with this factor are TA and K. This component is due to weathering and anthropogenic contamination.

3.6 Irrigation Water Assessment

By lowering osmotic pressure in plant structure cells, excessive dissolved ion concentrations in irrigation water have a physical and chemical impact on plants and agricultural soil. Therefore, the electrical conductivity (EC), percent sodium absorption ratio (SAR), sodium (percent Na+), permeability index (PI), residual sodium carbonate (RSC), magnesium ratio (MR), and Kelly ratio are frequently used to determine the danger of salinity (KR). The results are shown in Table 17 and the comparison of these indices to the common criteria is shown in Table 18.

Electrical conductivity was used to compute the salinity risk (C), which ranged from 149 to 391 S/cm (234 S/cm), suggesting a low salinity hazard that is safe for irrigation. A crucial chemical indicator for determining how suitable a water source is for irrigation is the salt content or alkali hazard for crops, which is expressed in sodium adsorption ratio. Important calcium and magnesium ions are those that tend to offset the effects of sodium. When SAR concentrations are too high, the physical structure of the soil is destroyed [23]. Soil particles absorb sodium, which is then bound to them. When dry, the soil becomes compact and hard, making it impenetrable to water penetration. A risk occurs when sodium replaces the adsorbents that hold calcium and magnesium because it weakens the structure of the soil. The analyzed water samples' percent SAR ranges from 34.39 to 86.44. (63.72 avg.). Generally speaking, the values are unsuitable for irrigation when using the average value. The percent Na+ is inversely proportional to permeability of soils. The range of the percent Na+ obtained, which corresponds to excellent water, is 16.09 to 39.33 (28.86 on average). Additionally, the Wilcox plot [63] of the water samples (Fig. 12) demonstrates that the irrigation water is "excellent to good."

Na^+, Ca^{2+}, Mg^{2+}, HCO_3^- and Cl^- concentrations have a big impact on permeability. It is very crucial for plant growth. Plant growth is inhibited when permeability in the soil zone is low. The degree of permeability in the soil is measured using the permeability index (PI). Permeability index is a word used to describe the soil's degree of permeability (PI) The water samples' PI ranges

from 22 to 45. (35 avg.). The groundwater samples fall into the "suitable - marginal" group, taking the average value, it means that the groundwater is marginal or moderate for irrigation, according to the classification of PI in Table 16. The difference between carbonates (HCO_3^- + CO_3^{2-}) and alkaline earths (Ca^{2+} + Mg^{2+}), which is measured in meq/l, is known as residual sodium carbonate (RSC). Alkaline earths that are precipitated by carbonates have an impact on water quality by raising the percentage of Na^+. This is more prevalent when carbonates are present in excess compared to alkaline earths. The excess carbonates combine with Na^+ to form $NaHCO_3$, which affects soil structure. The RSC values range between -4 to -1 (-2.3 avg.). Therefore, on the basis of RSC, the irrigation water quality in the area is generally "marginal/suitable".

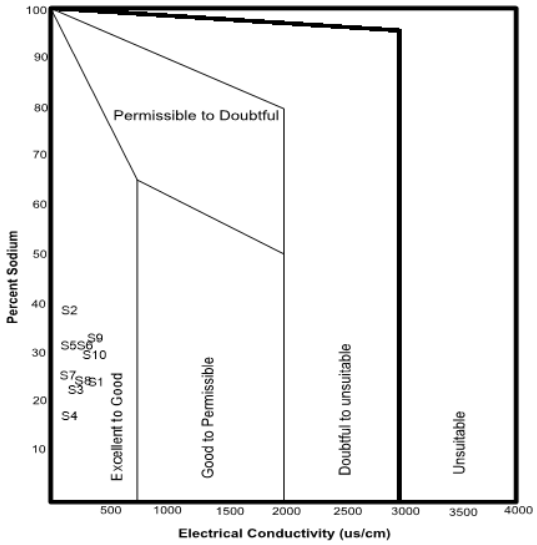

Figure 12. Wilcox Plot of Sampled water

Table 15. Correlation matrix of chemical parameters in water samples from the study area

Parameter	TA	TH	HCO_3	Ca	Mg	Cl	Na	K	SO_4	NO_3	Fe	Mn
TA	1											
TH	0.16	1										
HCO_3	0.18	0.15	1									
Ca	0.36	0.87	0.32	1								
Mg	-0.03	0.09	-0.17	0.06	1							
Cl	0.30	0.85	0.38	0.87	0.10	1						
Na	0.05	0.72	0.05	0.62	0.10	0.62	1					
K	0.38	0.10	0.24	0.40	-0.35	0.46	-0.09	1				
SO_4	-0.39	0.08	-0.14	-0.23	-0.06	-0.10	0.01	-0.57	1			
NO_3	-0.08	0.23	0.08	0.18	-0.64	0.06	-0.20	0.12	0.38	1		
Fe	0.36	-0.02	0.61	0.07	-0.14	-0.08	-0.16	-0.13	-0.24	0.23	1	
Mn	0.13	0.56	0.58	0.62	-0.21	0.60	0.41	0.34	-0.42	0.25	0.53	1

Table 16. Varimax orthogonal rotated factor loadings from PCA of the Analyzed parameters

Variable	Factor 1	Factor 2	Factor 3	Factor 4
TA	0.13	0.24	-0.08	0.61
TH	0.96	0.06	0.07	-0.07
HCO_3	0.19	0.77	0.12	0.17
Ca	0.89	0.15	0.07	0.28
Mg	0.12	-0.09	-0.86	-0.12
Cl	0.91	0.06	0.04	0.27
Na	0.82	-0.04	-0.23	-0.11
K	0.18	-0.13	0.38	0.87
SO_4	0.04	-0.21	0.26	-0.84
NO_3	0.10	0.15	0.90	-0.22
Fe	-0.13	0.96	0.06	0.05
Mn	0.56	0.62	0.20	0.26
Eigen value	3.67	2.08	1.89	2.16
% Variance	31.0	17.0	16.0	18.0
Cumulative % variance	37.0	81.0	100.0	59.0
Interpretation of process	Mineral dissolution, Weathering and anthropogenic pollution	Mineral dissolution and precipitation	Organic matter degradation and anthropogenic pollution	Weathering/anthropogenic pollution

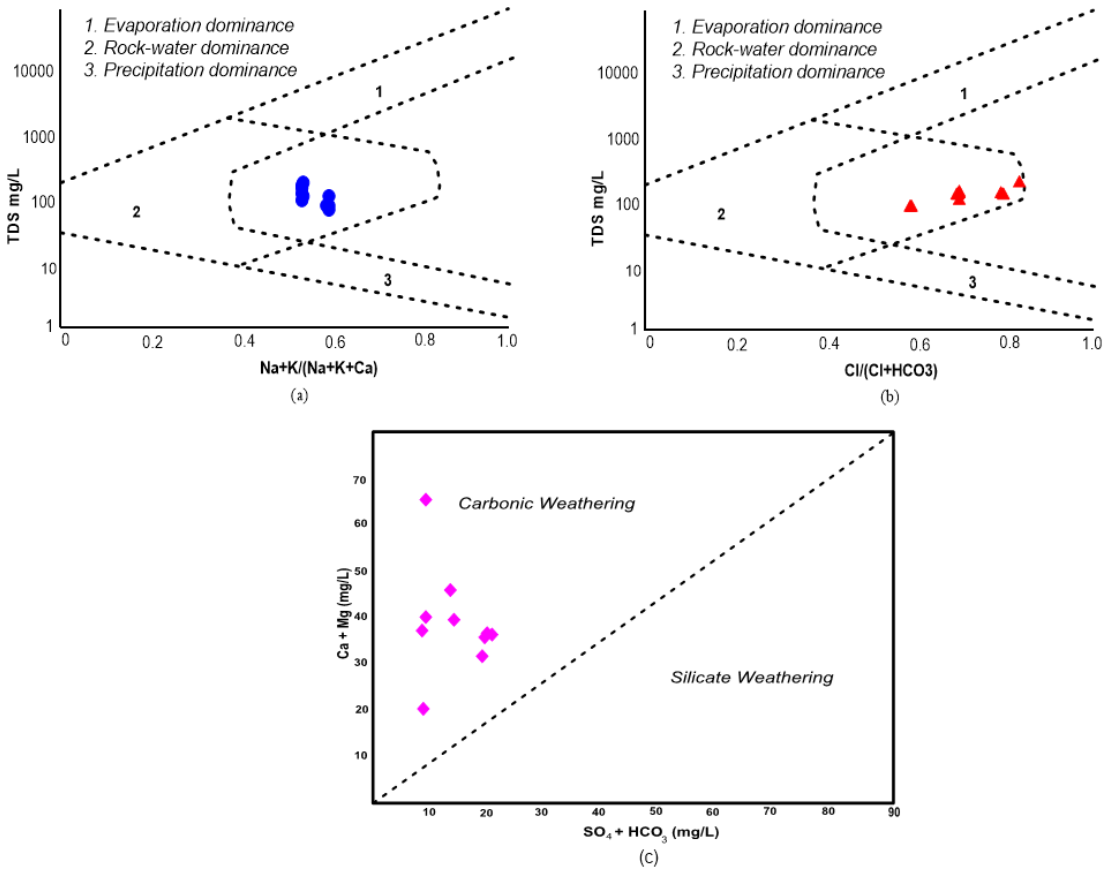

Figure 10. Mechanisms controlling groundwater chemistry in the study area showing a mixed domain (a&b) and (c) carbonic weathering prevalence

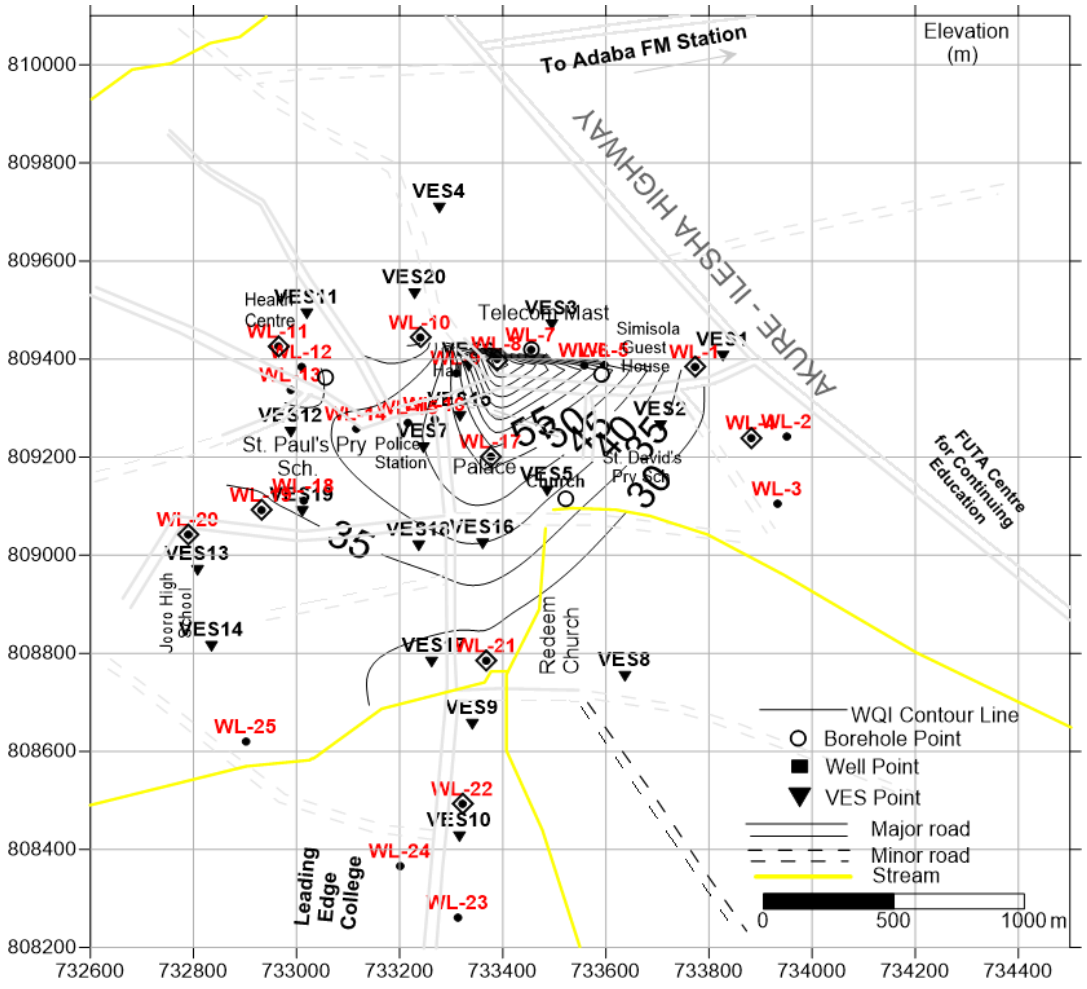

Figure 11. The distribution of WQI values across the study area

Table 17. Results of the Irrigation Indices/parameters obtained from the well water samples

Well No.	PI (%)	RSC	MR	KR	%SAR	%Na	EC
WL-1	27	-4	47	0.26	74.39	25.51	391
WL-4	45	-1	42	0.39	60.99	39.33	149
WL-8	32	-2	43	0.26	55.94	26.62	204
WL-10	22	-3	74	0.13	34.39	16.09	162
WL-12	40	-2	35	0.33	65.83	32.33	236
WL-17	42	-2	26	0.37	73.46	32.98	262
WL-19	28	-2	47	0.22	48.34	25.53	242
WL-20	33	-2	64	0.24	52.31	25.14	198
WL-21	44	-2	52	0.42	85.14	33.67	205
WL-22	37	-3	57	0.38	86.44	31.38	290

Table 18. Irrigation Indices and their categorization [23]

Parameter	Sample range	Classification
Na% (meq/l)	0 – 20	Excellent
	20 – 40	Good
	40 – 60	Permissible
	60 – 80	Doubtful
	>80	Unsuitable
SAR (meq/l)	0 – 10	Excellent (suitable for all types of crops and soil except for those crops sensitive to Na
	10 – 18	Good (suitable for coarse textured or organic soil with permeability
	18 – 26	Fair (harmfully for almost all soils)
	>26	Poor (unsuitable for irrigation)
RSC (meq/l)	<1.25	Good
	1.25 – 2.50	Medium
	>2.50	Bad
EC (μs/cm)	<250	Low salinity hazard (good)
	250 – 750	Medium salinity hazard (moderate)
	750 – 2250	High salinity hazard (poor)
	>2250	Very high salinity hazard (very poor)
PI (meq/l)	>75%	Suitable
	25 – 75%	Marginal
	<25%	Unsuitable
MR (meq/l)	<50	Suitable
	>50	Unsuitable
KR (meq/l)	<1.0	Good
	>1.0	Not Good

The magnesium ratio is a proportion that compares magnesium to alkaline earths (Ca^{2+} + Mg^{2+}). Magnesium degrades soil structure in water with high salinity and higher Na^{+}. More Mg^{2+} can make soil more acidic in equilibrium, which has an impact on crop production [4]. The water samples have MRs that range from 26 to 74 (48.7 on average) and are appropriate for irrigation. Kelly ratio, which compares the concentration of Na^{+} to that of Ca^{2+} and Mg^{2+}, is used to categorize the quality of irrigation water. If the KR is less than one, irrigation is appropriate; if it is greater than one, irrigation is not appropriate. The computed KR values for the water samples range from 0.13 to 0.42. (0.3 avg.)

3.7 Groundwater potential index value

Therefore, using multi criteria parameters as rated in Table 19, where all the measured parameters are rated and weighted based on their significances in groundwater accumulation. The parameters were derived from VES, borehole logging, pumping test and hydraulics measurement. The summation of these parameters resulted into generation of groundwater potential index values (GWPIV) which was used in developing groundwater potential map for the area. All the parameters: weathered layer thickness (WT), weathered layer resistivity (WR), overburden thickness (OT), traverse resistance (TR), transmissivity (TM), reflection coefficient (RC), fracture contrast (FC), formation factor (FM), water quality index (WQI), aquifer vulnerability index (AVI), and longitudinal conductance (LC) were summed up (equation 21) by attaching different weights (w) and ratings (r) based on their significance on groundwater accumulation/storage and exploitation.

$$GW = f(WT, WR, OT, TR, TM, RC, FC, LC, AVI)$$

Therefore, the GWPIV was determined using Eq. 21.

$$\text{GWPIV} = WT_w WT_r + WR_w WR_r + OT_w OT_r + TR_w TR_r + TM_w TM_r + RC_w RC_r + FC_w FC_r + LC_w LC_r + AVI_w AVI_r \quad (21)$$

The GWPIV obtained ranges from 112 – 171 with an average of 130 indicating a low potential. The developed groundwater potential map (Fig. 13) showed predominant low potential across the study except a small zone in the northeast which showed better hydrogeological prospect.

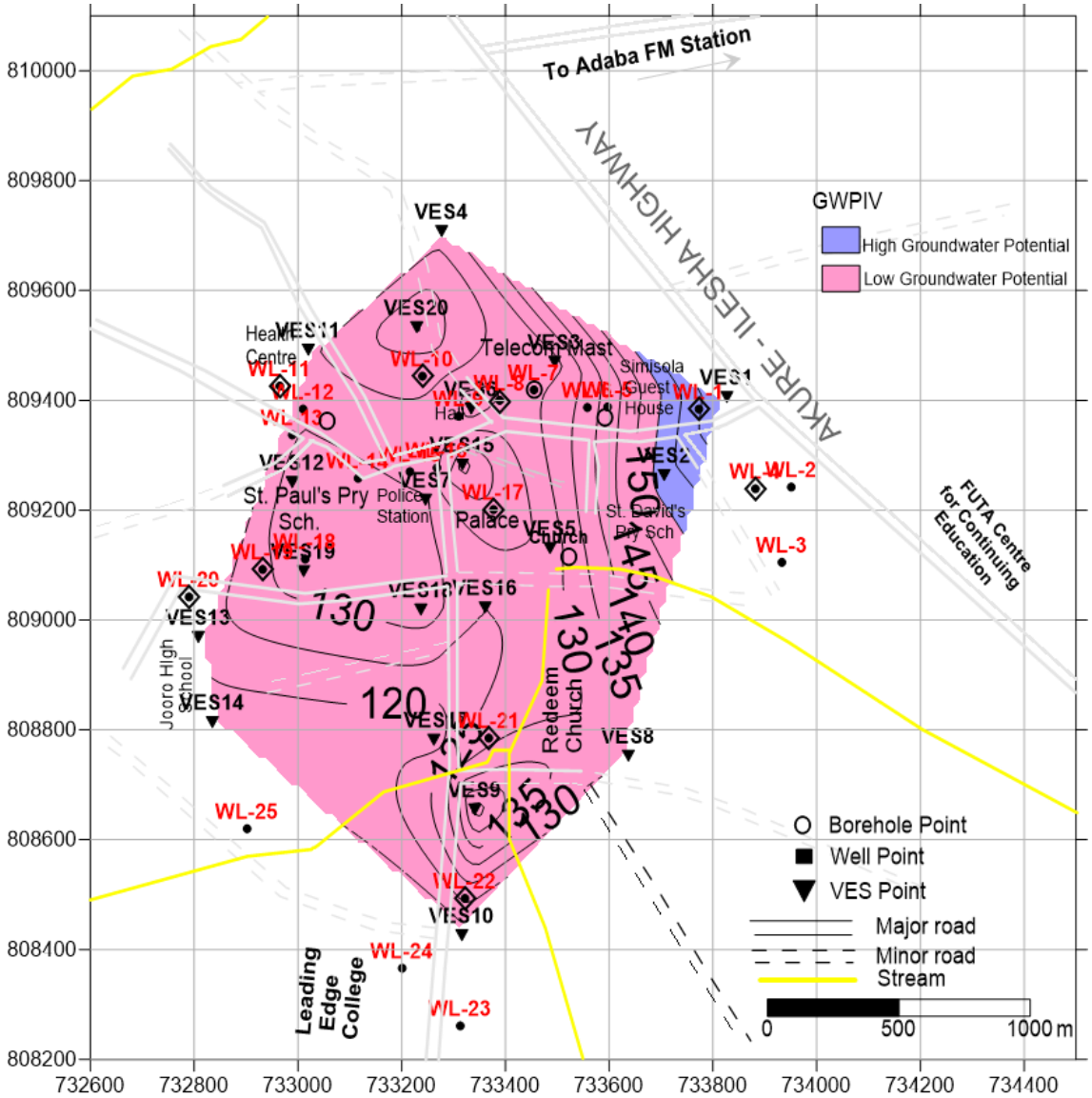

Figure 13. Groundwater Potential map developed for the study area using GWPIV

4. Conclusion

Findings revealed maximum of five geologic sequence comprising topsoil (25–222 ohm-m), thicknesses (0.5 – 1.2 m), composed of clay, and sandy clay; a layer composed of clay/sandy clay/clay sand (33-320 ohm-m), thicknesses (2.2 – 7.5 m); the weathered layer, which is composed of clay/sandy clay and clayey sand (29–365 ohm-m), thicknesses (2.3 – 17.5 m); the partly weathered/fractured layer (25–412 ohm-m), thicknesses (6.1 – 11.5 m); and the fresh basement (221–9540 ohm-m). The depth to the basement rocks ranged from 5.7 to 32.5 m. The overburden thickness ranges from 5.7 to 32.5 m. The weathered layer and the fractured basement are the main water bearing units in the research region, according to the groundwater assessment of Ibulesoro. In most locations, the aquifer system is unconfined, meaning that the saturated thickness is equal to the difference between the free water table and the aquiclude. It is more prevalent where there is a combination of the two. As a result, the saturated thickness of an unconfined aquifer is not constant but rather variable due to changes in the water table's position over time. The obtained K and T for the aquifers ranged from 0.13 – 0.84 m/d and 0.77 – 16.9 m^2/d respectively. The measured pore water resistivity varied from 34.84 – 53.48 ohm-m, while groundwater formation factor (Fm) ranged from 0.59 to 11.33. The groundwater's physicochemical and biological characteristics met the World Health Organization's requirements for potable water. The groundwater's irrigation indices also met requirements for being acceptable for irrigation, with the exception of RSC, which is over the advised standard. The groundwater was rated by the GWPIV as low and extremely prone to contamination. Ca-Mg-Cl-mixed water is the most common form. The study has contributed to knowledge by given baseline information about aquifer

characteristics, in order to enhance the success rate of borehole drilling and groundwater development in the area. However, the limitation experienced in the course of data acquisition was that, the area was built-up, consequently this limitation did not allow extensive spread/stretch of the current electrodes during VES survey. Therefore, this calls for other methods adaptable and versatile to groundwater investigation in rugged or built-up area, such as seismic method, remote sensing (which can further help in understanding the fault/fracture), borehole logging (e.g., caliper logging), ground penetrating radar. These methods integrated with GIS are recommended for further studies.

Table 19. Muti-criteria Parameters and its probability rating and weights for selected measured parameters in relation to groundwater evaluation

1	**Parameter**	Range	Weight	Remark	Rating
	Weathered Layer	0 – 10	1	Low	
	Thickness (m)	10 – 20	2	Moderate	0.06
		>20	3	High	
2	Weathered Layer	0 – 100	1	Very Poor	
	Resistivity (ohm-m)	100 – 200	2	Poor	0.06
		200 - 300	3	Moderate	
		>300	5	Good	
3	Overburden	0 – 15	1	Low	
	Thickness (m)	15 – 30	2	Medium	0.09
		>30	4	High	
4	Transverse	0 – 5000	1	Low	
	Resistance	5000 – 10000	3	Fair	0.06
		>10000	5	High	
5	Transmissivity	0 – 10	1	Low	
		10 – 20	2	Moderate	0.11
		>20	3	High	
6	Reflection	<0.1	3	High	
	Coefficient	0.1 – 0.5	2	Moderate	0.04
		0.5 – 1.0	1	Low	
7	Fracture Constrast	0 - 20	3	High	
		20 – 50	2	Moderate	0.04
		>50	1	Low	
8	Apparent	0 – 3	1	Low	
	Formation Factor	3 – 5	3	Fair	0.04
		>5	5	Good	
9.	Longitudinal	0.10 – 0.50	1	High	0.50
	Conductance				
		0.50 – 0.75	3	Moderate	
		0.75 – 1.0	5	Low	
10	Aquifer	<1 - 2	1	Extremely high	
	vulnerability index	2 – 3	3	Moderate	0.50
		>3	5	Extremely low	

Acknowledgement

The author is grateful to Federal Water Resources, Akure, Ondo State, Nigeria for assistance rendered during analysis of water samples.

Author contributions

Olumuyiwa Olusola Falowo: Conceptualization, Methodology, Software, Field study, Visualization, Investigation, Writing-Reviewing, Editing, and Data Analysis. **Abayomi Solomon Daramola:** Data curation, Writing-Original draft preparation, Software, Validation., Field study, Data interpretation, and Proof-reading

Conflicts of interest

The authors declare no conflicts of interest.

References

1. Hordon, R. M. (1977). Water supply as a limiting factor in developing communities; endogenous Vs. exogenous sources. Water resources Bulletin, 13: 933-939.
2. Sellers, J. H. (1973). Tax implications of groundwater depletion. Groundwater, 11, 4, 27-35.
3. Dalila, Z., Boudoukha, A., Abderrahmane, B., & Lahcen, B. (2017). Water Quality Assessment for Drinking and Irrigation Using Major Ions Chemistry in The Semiarid Region: Case of Djacer Spring, Algeria, Asian Journal of Earth Science, 10:9-21. https://doi.org/10.3923/Ajes.2017.9.21
4. Collins, R., & Jenkins, A. (1996). The Impact of Agricultural Land Use on Stream Chemistry in the Middle Hills of the Himalayas, Nepal. Journal of

Hydrology, 185, 71-86. http://doi.org/10.1016/0022-1694(95)03008-5
5. Davis, S. N., & Dewiest, R. J. M. (1967). Hydrogeology, John Wiley and Sons, 463.
6. Domenico, P. A., & Schwartz, F. W. (1990). Physical and Chemical Hydrogeology. John Wiley & Sons, New York, 824.
7. Fetter, C. W. (1990). Applied Hydrogeology, 2nd Edition CBS Publisher & Distributor, 592.
8. Ndatuwong, L. G., & Yadav, G. S. (2015). Application of geo-electrical data to evaluate groundwater potential zone and assessment of overburden protective capacity in part of Sonebhadra district, Uttar Pradesh. *Environmental earth sciences*, *73*(7), 3655-3664. http://doi.org/10.1007/s12665-014-3649-z.
9. Akinrinade, O. J., & Adesina, R. B. (2016). Hydrogeophysical investigation of groundwater potential and aquifer vulnerability prediction in basement complex terrain–a case study from Akure, Southwestern Nigeria. *Materials and Geoenvironment*, *63*(1), 55-56. http://doi.org/10.1515/rmzmag-2016-0005
10. Bayewu, O. O., Oloruntola, M. O., Mosuro, G. O., Laniyan, T. A., Ariyo, S. O., & Fatoba, J. O. (2017). Geophysical evaluation of groundwater potential in part of southwestern Basement Complex terrain of Nigeria. *Applied Water Science*, *7*(8), 4615-4632. https://doi.org/10.1007/s13201-017-0623-4
11. Egbueri, J. C. (2018). Assessment of the quality of groundwaters proximal to dumpsites in Awka and Nnewi metropolises: a comparative approach. *International journal of energy and water resources*, *2*(1), 33-48. https://doi.org/10.1007/S4210 8-018-0004-1
12. Selvam, S. (2016). 1D Geoelectrical Resistivity Survey for Groundwater Studies in Coastal Area: A Case Study from Pearl City, Tamil Nadu. Journal of the Geological Society of India, 87, 169-178. http://dx.doi.org/10.1007/s12594-016-0385-x
13. Mogaji, K. A., & Omobude, O. B. (2017). Modeling of geoelectric parameters for assessing groundwater potentiality in a multifaceted geologic terrain, Ipinsa Southwest, Nigeria – A GIS-based GODT approach, NRIAG Journal of Astronomy and Geophysics, 6:2, 434-451. https://doi.org/10.1016/j.nrjag.2017.07.001
14. Telford, W. M., Geldart, L. P., Sheriff, R. E., & Keys, D. A. (1976). Applied Geophysics. Cambridge University Press, London, U. K.
15. Walton, W. C. (1991). Principles of Groundwater Engineering. Lewis Publishers, Inc., Chelsea, MI.
16. Obiora, D. N., Ibuot, J. C., & George, N. J. (2016). Evaluation of aquifer potential, geoelectric and hydraulic parameters in Ezza North, southeastern Nigeria, using geoelectric sounding. *International journal of environmental science and technology*, *13*(2), 435-444. https://doi.org/10.1007/s13762-015-0886-y
17. Anomohanran, O. (2013). Geophysical Investigation of Groundwater Potential in Ukelegbe, Nigeria. Journal of Applied Sciences, 13, 119-125. http://dx.doi.org/10.3923/jas.2013.119.125
18. Hussain, Y., Ullah, S. F., Hussain, M. B., Martinez-Carvajal, H., & Aslam, A. Q. (2016). Protective Capacity Assessment of Vadose Zone Material by Geo-Electrical Method: A Case Study of Pakistan. International Journal of Geosciences, 7, 716-725. http://dx.doi.org/10.4236/ijg.2016.75055
19. Hamill, L., Bell, F.U. (1986). Groundwater Resources Development. Britain Library Cataloguing in Publication Data London, 151 – 158.
20. Kruseman, G. P., & de Ridder, N. A. (1994). Analysis and Evaluation of Pumping Test Data, International Institute for Land Reclamation and Improvement, AA Wageningen, The Netherlands, Second Edition (Completely Revised).
21. Logan, J. (1964). Estimating transmissivity from routine production tests of water wells. Groundwater, 2(1), 35-37. https://doi.org/10.1111/j.1745-6584.1964.tb01744.x
22. El-Naqa, A., & Al-Shayeb, A. (2009). Groundwater Protection and Management Strategy in Jordan. Water Resources Management, 23, 2379-2394. https://doi.org/10.1007/s11269-008-9386-x
23. Singh, S. N., Janardhana, R., & Ramakrishna, Ch., (2015). Evaluation of Groundwater Quality and its Suitability for Domestic and Irrigation Use in Parts of the Chandauli-Varanasi Region, Uttar Pradesh, India Journal of Water Resource and Protection, 7, 572-587. http://dx.doi.org/10.4236/jwarp.2015.77046
24. Rao, N. S. (2017). Hydrogeology- Problems with Solutions. PHI Learning Private Limited, 265.
25. Paramaguru, P., Anandhan, P., Chidambaram, S., Ganesh, N., Nepolian, M., Devary, N., Vesudevan, U., Rakesh, R. G., & Pradeep K. (2016). Appraisal of Groundwater Quality in the Cuddalore District of TN, India, International research journal of earth sciences, 4(6), 23-30.
26. Walski, T. M., & Parker, F. L. (1974). Consumers' water quality index. Journal of the Environmental Engineering Division, 100, 259–611.
27. Hem, J. D. (1989). Study and Interpretation of the chemical characteristics of natural waters. U.S. Geological survey water supply paper 2254, 3rd Edition.
28. Napolitano, P., & Fabbri, A. (1996). Single-Parameter Sensitivity Analysis for Aquifer Vulnerability Assessment Using DRASTIC and SINTACS. In: HydroGIS 96: Application of Geographical Information Systems in Hydrology and Water Resources Management, Proceedings of Vienna Conference, IAHS Pub., Vienna, 235, 559-566. http://hydrologie.org/redbooks/a235/iahs_235_0559.pdf
29. Aller, L., Bennet, T., Leher, J. H., Petty, R. J., & Hackett, G. (1987). DRASTIC: A Standardized System for Evaluating Groundwater Pollution Potential Using Hydro Geological Setting. EPA, 35, 600-622. https://link.springer.com/article/10.1007/s11269-008-9319-8
30. Zhu, X., & Ierland, E. C. V. (2012). Economic modeling for water quantity and quality management: A welfare program approach, Water Resource Management, 26, 2491–2511

31. Dalkey, N. C. D. (1968). An objective water quality index, The Rand Corporation Harkins. Journal - Water Pollution Control Federation, 46, 588–591.
32. Satheesh, B., Sateesh, S., Kumar, K., & Reddy, N. (2017). Assessment of Groundwater Quality for Irrigation Use and Evolution of Hydrochemeical Facies in the Yeshwanthapur Sub-Basin, Warangal Dist. IOSR Journal of Applied Geology and Geophysics (IOSR-JAGG), 5(4) Ver. I, 14-20. https://doi.org/ 10.9790/0990-0504011420
33. Harkins, R. D. (1974). An objective water quality index. Journal–Water Pollution Control Federation, 46, 588–591.
34. Couillard, D., & Lefebvre, Y. (1985). Analysis of water quality indices. Journal of Environmental Management, 21, 161–179.
35. Brutsaert, W., Gross, G. W., & Mc Gehee, R. M. (1975). C.E. Jacob's study on the prospective and hypothetical future of the minning of the groundwater deposited, 13; 492-505.
36. Coulibaly, H., & Rodriguez, M. J. (2004). Development of performance indicators for Quebec small water utilities. Journal of Environmental Management, 73(3), 243–255. https://doi.org/ 10.1016/j.jenvman.2004.07.003
37. Gass, T. E., & Lehr, J. (1977). Groundwater energy and the groundwater heat pump. Water well journal, 31(4), 42-47.
38. Khrisat, H. T., & Al-Bakri, J. (2019). Assessment of Groundwater Vulnerability in Azraq Catchment in Fuhais-Jordan Using DRASTIC Model. Open Journal of Geology, 9, 364-377. https://doi.org/10.4236/ojg.2019.97024
39. Jain, C. K., Bandyopadhyay, A., & Bhadra, A. (2010). Assessment of Ground Water Quality for Drinking Purpose, District Nainital, Uttarakhand, India. Environmental Monitoring and Assessment, 166, 663-676. http://doi.org/10.1007/s10661-009-1031-5
40. Saeedi, M., Abessi, O., Sharifi, F., & Meraji, H. (2009). Development of groundwater quality index. Environ Monit Assess, 10pp. http://doi.org/10.1007/S10661-009-0837-5.
41. Rao, G. S., & Nageswararao, G. (2013). Assessment of ground water quality using water quality index. *Archive of Environmental Sciences*, *7*(1), 1-5.
42. Kalaivanan, K., Gurugnanam, B., Pourghasemi, H. R., Suresh, M., & Kumaravel, S. (2017). Spatial Assessment of Groundwater Quality Using Water Quality Index and Hydrochemical Indices in the Kodavanar Sub-Basin, Tamil Nadu, India. Sustain Water Resour Manag. https://doi.org/10.1007/S4089 9-017-0148-X
43. Li, P., Qian, H., & Wu, J. (2010). Groundwater Quality Assessment Based on Improved Water Quality Index in Pengyang County, Ningxia, Northwest China. E-Journal of Chemistry. 7(S1): S209-S216. https://doi.org/ 10.1155/2010/451304
44. Ojo, J. S., Olorunfemi, M. O., Aduwo, I. A., Bayode, S., Akintorinwa, O. J., Omosuyi, G. O., & Akinluyi, F.O. (2014). Assessment of surface and groundwater quality of the Akure metropolis, Southwestern Nigeria. Journal of Environment and Earth Science, ISSN 2225-0948, 4(23), 19.
45. NIMET. (2012). Nigeria Meterological Agency. Nigeria Climatic Data: Abuja, Nigeria. www.nimetng.org
46. Nigeria Geological Survey Agency (NGSA). (2006). Published by the Authority of the Federal Republic of Nigeria.
47. Orellana, E., & Mooney, H. M. (1966). Master Tables and Curves for Vertical Electrical Sounding over Layered Structures. Interciencia, Madrid, Spain.
48. Zohdy, A. A. R., Eaton, G. P., & Mabey, D. R. (1974). Application of surface geophysics to groundwater investigations. United State Geophysical Survey, Washington.
49. Loke, M. H. (1997). Electrical Imaging surveys for Environmental and Engineering Studies. A partial guide to 2-D and 3-D surveys. Minden Heights, 11700, Penang, Malaysia.
50. Gibb, J. P., Schuller, R. M., Griffin, R. A. (1981). Procedures for the Collection of Representative Water Quality Data from Monitoring Wells. Cooperative Groundwater Report No. 7, Illinois State Water Survey and Illinois State Geological Survey, Champaign, Illinois.
51. APHA, (1998). America Public Health Association. Standard Methods for the Examination of Water and Waste Water. 18th Edition, Washington D. C, 4-17.
52. Kakati, S. S., & Sarma, H. P. (2007). Studies on water quality index of drinking water of Lakhimpur District. *Indian Journal of Environmental Protection*, *27*(5), 425-428.
53. Haque, S., Sadique, A. B. M., Mazharul, M. I., Zakia, S., Nargis, A., & Masud, H. (2017). Assessment of Irrigation Water Quality of Pabna District (North-Western Part) of Bangladesh for Securing Risk-Free Agricultural Production, American Journal of Water Science and Engineering, 3(6), 67-71. http://doi.org/10.11648/j.ajwse.20170306.11
54. Bell, F. G. (2007). Engineering Geology, Second Edition. Elsevier, 581pp.
55. Mgbenu, C. N., & Egbueri, J. C. (2019). The hydrogeochemical signatures, quality indices and health risk assessment of water resources in Umunya district, southeast Nigeria. Appl Water Sci. https://doi.org/10.1007/s1320 1-019-0900-5
56. Raju, N. J., Ram, P., & Dey, S. (2009). Groundwater Quality in the Lower Varuna River Basin, Varanasi District, Uttar Pradesh, India. Journal of the Geological Society of India, 7, 178-192. http://dx.doi.org/10.1007/s12040-008-0048-4
57. Vasanthavigar, M., Srinivasamoorth, K., Vijayaragavan, K., Rajiv, G. R., Chidambaram, S., Anandhan, P., Mani, V. R., & Vasudevan, S. (2010). Application of Water Quality Index for Groundwater Quality Assessment: Thirumanimuttar Sub-Basin, Tamilnadu, India. Environmental Monitoring and Assessment, 171, 595-609. http://dx.doi.org/10.1007/s10661-009-1302-1
58. WHO, (2011). Guidelines for Drinking Water Quality, 3rd Ed. World Health Organization, Geneva, 2011.
59. Egbueri, J. C., Mgbenu, C. N., & Chukwu, C. N. (2019). Investigating the hydrogeochemical processes and quality of water resources in Ojoto and environs using

integrated classical methods. Model Earth Syst Environ. https://doi.org/10.1007/s40808-019-00613–y
60. Igbemi, A., Nwaogazie, I. L., Akaranta, O., & Abu, G. O., (2019). Water Quality Assessment by Pollution Indices in Eastern Obolo Coastline Communities of Nigeria. American Journal of Water Resources, 7(3), 111-120. http://doi.org/10.12691/ajwr-7-3-4
61. Ochungo, E. A., Ouma, G. O., Obiero, J. P. O., & Odero, N. A. (2019). Water Quality Index for Assessment of Potability of Groundwater Resource in Langata Sub County, Nairobi-Kenya. American Journal of Water Resources, 7(2), 62-75. http://doi.org/10.12691/ajwr-7-2-4.
62. Piper, A. M. (1953). A Graphic Procedure in the Chemical Interpretation of Water Analysis. US Geological Survey Groundwater Note, 12.
63. Wilcox, L. V. (1948). Classification and Use of Irrigation Waters. U.S. Department of Agriculture, Washington Dc, 962.